NASA CR-139177

(NASA-CR-139177) OPTICAL IMAGE OF A COMETARY NUCLEUS: 1980 FLYBY OF COMET ENCKE (Lockheed Missiles and Space Co.) 61 p HC $4.25 CSCL 03A

N75-17258

Unclas

G3/89 09841

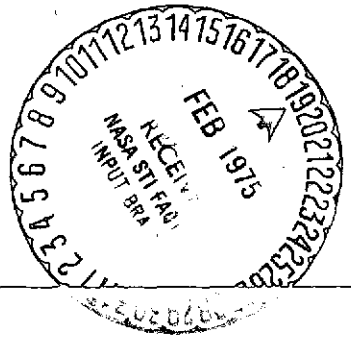

Lockheed

MISSILES & SPACE COMPANY

A GROUP DIVISION OF LOCKHEED AIRCRAFT CORPORATION

SUNNYVALE, CALIFORNIA

OPTICAL IMAGE OF A COMETARY NUCLEUS: 1980 FLYBY OF COMET ENCKE

W. C. Wells
R. S. Benson
A. D. Anderson
G. Gal

August 1974

Contract NAS5-20566

Radiation Physics Laboratory
Palo Alto Research Laboratory
Lockheed Missiles and Space Company
Subsidiary of Lockheed Aircraft Corporation
Palo Alto, Calif. 94304

TABLE OF CONTENTS

LIST OF FIGURES

LIST OF TABLES

I. INTRODUCTION

This is a study of the feasibility of obtaining optical images of a cometary nucleus via a flyby of Comet Encke. This study is based on a physical model of the dust cloud surrounding the nucleus. Development of the model is based on available physical data and theoretical knowledge of cometary physics. Using this model, calculations are made of the absolute surface brightness of the dust in the line of sight of the on-board camera and the relative surface brightness of the dust compared to the nucleus. The brightness is calculated as a function of heliocentric distance and for different phase angles (sun-comet-spacecraft angle).

The study of the feasibility of obtaining optical images of the nucleus of Comet Encke via a flyby was divided into two parts. First a physical model of the dust cloud surrounding the nucleus was derived and then our Mie scattering code was employed to calculate the absolute brightness of the dust in the line of sight of the on-board camera. The surface brightness of the comet was compared to this background brightness along with contributions from debris and ice particles. Conclusions were then drawn in light of these results regarding the optimum imaging system for a flyby mission.

II. BACKGROUND OF FLYBY MISSIONS

At a symposium on the exploration of space held in Washington, D.C. in April 1959, Whipple (1959) pointed to the possibility of sending a space probe through the neighborhood of a comet. Two years later, Swings (1962) gave an extended survey on the scientific objectives and feasibility of such a mission at a symposium held in Pasadena, Calif. in August 1961.

He summarized the existing knowledge about comets and pointed to those problems in the physics of the comets for which investigations by means of space probes would be of special value.

There are quite a few problems which would be handled best with instruments installed in a cometary probe (Lust, 1969):

(a) The structure and composition of the nucleus, its surface temperature and its color.

(b) Chemical processes related to the formation of the observed radicals which take place in the vicinity of the nucleus where the density is high, and the ejection velocity of the different particles.

(c) The composition of the cometary atmosphere, the mechanisms of dissociation and ionization, the size and nature of the dust grains.

(d) The density gradient and partial densities of the different constituents in the coma and in the tail.

(e) The interaction with the solar wind and with interplanetary magnetic fields, the structure of shock fronts and related problems of plasma physics and magneto-hydrodynamics.

Among the questions which have to be solved in the preparation of a cometary probe is which comet should be selected for a first space mission. Much work has been put into this problem by different groups in the U.S.A. and in Europe, and all these groups came to realize that the difficulties of such a mission are far greater than had first been anticipated. It is evident that a periodic comet which has been observed for many apparitions and whose orbit has been calculated with some accuracy is an easier target

than a new comet which suddenly appears without being predicted and whose path has to be calculated from a few observations taken in small time intervals. But there are other reasons why a periodic comet can be reached more easily by a space vehicle than a new one. The orbits of almost all periodic comets have relatively small inclination to the ecliptic plane, and a motion in the same sense as Jupiter and all other planets (direct orbit). The inclinations of the orbital planes of the new comets are, on the other hand, randomly distributed between 0 and 180°, so that on the average these comets spend only a small fraction of their time close to the ecliptic plane while they are passing through the nodes. This causes a severe restriction for the launch window, while retrograde motions (inclination between 90° and 180°) cause very large approach velocities of the spacecraft with respect to the comet. Expensive terminal guidance would therefore be necessary to force the trajectory of the spacecraft into or near to the orbital plane of the new comet and to diminish the relative velocity to a slow fly-by or to achieve a rendezvous.

Because of these difficulties, the new comets have been excluded as a first aim for a cometary probe by all groups who have investigated the feasibility of such a mission in spite of their high scientific interest.

Different groups in the U.S.A. as well as in Europe have carried out detailed feasibility studies during the last years. In 1961, a space mission to a comet was considered for the first time in NASA contracted studies of the Scientific and Technical Laboratories Inc. (Corben, 1962).

There exist about 50 periodic comets which have been observed during more than one perihelion passage, and an additional 30 comets with periods less than 20 years observed during one apparition only. About 5-7 of these comets appear on the average per year. A great amount of work and extensive calculations have been carried out by the different study groups to select among these comets the objects being fitted for a first mission. Several selection criteria had to be applied with respect to the following points:

(a) The position of the comet at the time of intercept must be known with very high accuracy, and it became more and more clear that this condition is a major constraint for a cometary mission. It seems desirable that the probe should approach within 1000 km. If costly midcourse corrections are to be avoided, the position of the comet must be predictable at the time of launch, that is several months before intercept, with this accuracy.

To secure the necessary accuracy in the calculation of the orbital elements, it is necessary to start with a well-known orbit calculated from previous apparitions and to apply corrections by means of new observations made after recovery. Perturbations by planets, especially by Jupiter, can be the reason for considerable changes of the orbit. Also secular perturbations caused by a mass loss of the comet and non-gravitational forces play a role in this respect. Especially the location of the comet in its orbit, that is the daily motion, is affected by such perturbations. Since small errors in the daily motion will add up and result in large errors

in the time of perihelion passage, the accuracy of this parameter is very important (Porter et al., 1965). It seemed, therefore, necessary to exclude all comets which had been observed during one apparition only, and also some of the remaining comets whose predicted orbits were not well enough established.

(b) In order to guarantee observations of the comet's position necessary for orbit corrections, the comet should be recovered at least 2 months before launch, and it should be seen against a dark sky for several hours per night. This imposes the condition that the comet must be at least of 20th magnitude -- the limit for recovery of an object whose position is known -- several months before perihelion passage. The average brightness of periodic comets is so small that not many of them fulfill this condition.

The question of the accuracy of cometary orbits has been investigated by the groups in the U.S.A. as well as the European ESRO group. The conclusion is that if every effort is made to recover a comet very early, that is about 20th magnitude, it should be possible to correct the predicted orbits to the accuracy necessary for a space mission for a number of comets.

(c) The comet should be bright enough at intercept to get photometric data and good quality spectra from ground-based observatories to supplement the spacecraft data. This means that the comet should be of 12th magnitude or brighter at the time of perihelion passage, and it should be seen against a dark sky for some hours. Since a great percentage of the periodic comets never become so bright, and since some of the brighter ones are in unfavorable positions on the sky near perihelion (close to the sun), this is a further restriction of the number of feasible comets.

(d) The ideal launch velocity should not exceed ~ 16 km/sec. This limit is chosen rather arbitrarily, it represents for instance the velocity required for a two year flight to Jupiter. It turned out, however, that this requirement does not impose a severe restriction, because almost every comet that was brighter than 12th magnitude at intercept fulfilled this condition.

(e) Of two otherwise equal missions, that which leads to a smaller relative approach velocity between spacecraft and comet and therefore allows for a longer stay of the spacecraft in the vicinity of the comet should have priority.

(f) All the points mentioned before refer more or less to the technical side of the mission. When choosing a comet, one should of course ask which mission promises the best scientific results. Comets are of very different activity according to their "age", that means according to the number of perihelion passages they have already made, because with every approach to the sun they lose a considerable amount of volatile material, and slowly get exhausted and inactive.

Summarizing the different points, a feasible comet should fulfill the following conditions:

(1) A reliable predicted orbit should be available.

(2) The comet should be of at least 20th magnitude 2 months before launch, and at that time be well observable for at least 2 hours per night.

(3) It should be of at least 12th magnitude at intercept, and distinctly visible from the earth.

(4) The launch velocity should not exceed $\sim$ 16 km/sec.

(5) The relative approach velocity between comet and spacecraft should be low.

(6) The comet should be interesting from a scientific point of view.

A mission to Comet Encke in 1980 meets these requirements and should be undertaken.

III. PHYSICAL PROPERTIES

With an estimate for the size of the nucleus of Comet Encke, and using the icy-conglomerate model, we estimate the distribution of non-volatile dust particles near the nucleus.

A. Nucleus

Although Whipple's (1950) model for comet nuclei is not universally accepted (e.g., Lyttleton, 1972), it has been used to successfully explain a number of cometary phenomena. Not the least of these is the non-gravitational force required to reproduce the orbital motion of Comet Encke and several other comets (Marsden and Sekanina, 1974 and earlier papers in this series). The non-gravitational acceleration derived by Marsden and Sekanina (1974) for Comet Encke shows a regular decrease which is consistent with the existence of a porous, rocky core, within which "dirty ice" is embedded (Sekanina, 1969b). Since the gravitational acceleration is proportional to the fractional rate of change of mass (as well as the degree of anisotropy of the ejection), it is necessary to estimate the mass of the nucleus in order to obtain the rate of mass loss itself. The mass (or mean density) and radius are also required in order to calculate the terminal velocities of ejected dust particles, since expanding vapor from the nucleus must lift the particles against gravitational attraction (Delsemme and Miller, 1971). Marsden and Sekanina (1971) estimate that Comet Encke loses 0.03 percent of its mass during each orbital revolution. A spherical nucleus of radius R_n = 1.7 km and mean density 1 g cm^{-3} has a mass $\sim 2 \times 10^{16}$ g, implying $\Delta M \sim 6 \times 10^{12}$ g per revolution; this mass loss is comparable to the estimates of Sekanina (1969a), which are $\sim 10^{13}$ g. If the geometric albedo of the nucleus is a_n = 0.1, then

$a_n R_n^2 \simeq 0.3$ km^2 which is to be compared with observed values which range from 0.24 (Roemer, 1966) to ≥ 0.82 km^2, which we derive from Roemer's (1972) observation of the apparent magnitude of Comet Encke at aphelion($m \simeq 20.5$). These lower limits result from our assumption that the comet was observed at opposition, thereby giving minimum earth-comet distance and phase angle. These results are consistent with the recent treatment of Delsemme and Rud (1973).

B. Non-Volatile Particles

1. Size Distribution

Lacking a determination of particle ejection for Comet Encke itself, we use the results of Finson and Probstein (1968) for Comet Arend-Roland and those of Sekanina and Miller (1973) for Comet Bennet. In particular, we use the distribution of particle sizes deduced by Finson and Probstein (1968), which they state is well-determined over the range $4 \leq \rho d \leq 40$ μm g cm^{-3}, where ρ is the bulk density of a particle of diameter d. We use the Sekanina and Miller (1973) distribution for the smallest particles (down to $\rho d = 0.9$μm g cm^{-3}). Specifically, denoting by n(a) da the number of particles with radii in the range a to a+da,

$$n(a) = \begin{cases} K_1(a/a_o)^{-5}(a-1)/a_o & 1 \leq a \leq 6.7\ \mu m \\ K_2(a/a_o)^{-3} & 6.7 \leq a \leq 14.4\ \mu m \\ K_3(a/a_o)^{-4} & 14.4 \leq a \leq 44.4\ \mu m \\ K_4(a/a_o)^{-5} & a > 44.4\ \mu m \end{cases}$$

The distribution for larger particles fits smoothly onto the distribution of interplanetary particles as given by Whipple (1968): $n \sim a^{-5}$. These are shown in Figure 1. The constant $a_o = 1$ μm, and the K's are determined by the requirement that

$$(4\pi\rho/3) \int_{a_o}^{\infty} a^3 n(a) da = 1 \text{ g}.$$

The rate of ejection of particles of radius a is then given by

$$P(a) = n(a) \frac{dM}{dt},$$

where dM/dt is the total mass-loss from the nucleus in the form of dust. We have

$$K_1 = 8.916 \times 10^{14}$$
$$K_2 = 1.137 \times 10^{14}$$
$$K_3 = 1.642 \times 10^{15}$$
$$K_4 = 7.298 \times 10^{16}.$$

The particle mass density is assumed to be $\rho = 0.45$ g cm^{-3}, which is approximately the value adopted by Whipple (1967, 1968) for meteroids of mass $m \geq 10^{-6}$ g. Super-Schmidt data for the Taurid meteor shower give a mean value of about 0.28 g cm^{-3} (Verniani, 1969). A somewhat higher density may be appropriate for the smaller particles: Whipple (1968) uses $\rho \simeq 1$ g cm^{-3} for $m \leq 10^{-6}$ g ($a \leq 175$ μm), and radio data for sporadic and shower meteors give $\rho \simeq 0.8$ g cm^{-3} (Verniani, 1973). The particle distribution would not be greatly changed if we were to use $\rho \simeq 1$ g cm^{-3}, except that n(a) would peak at $a \simeq 0.6$ μm and extend to about 0.55 μm. These

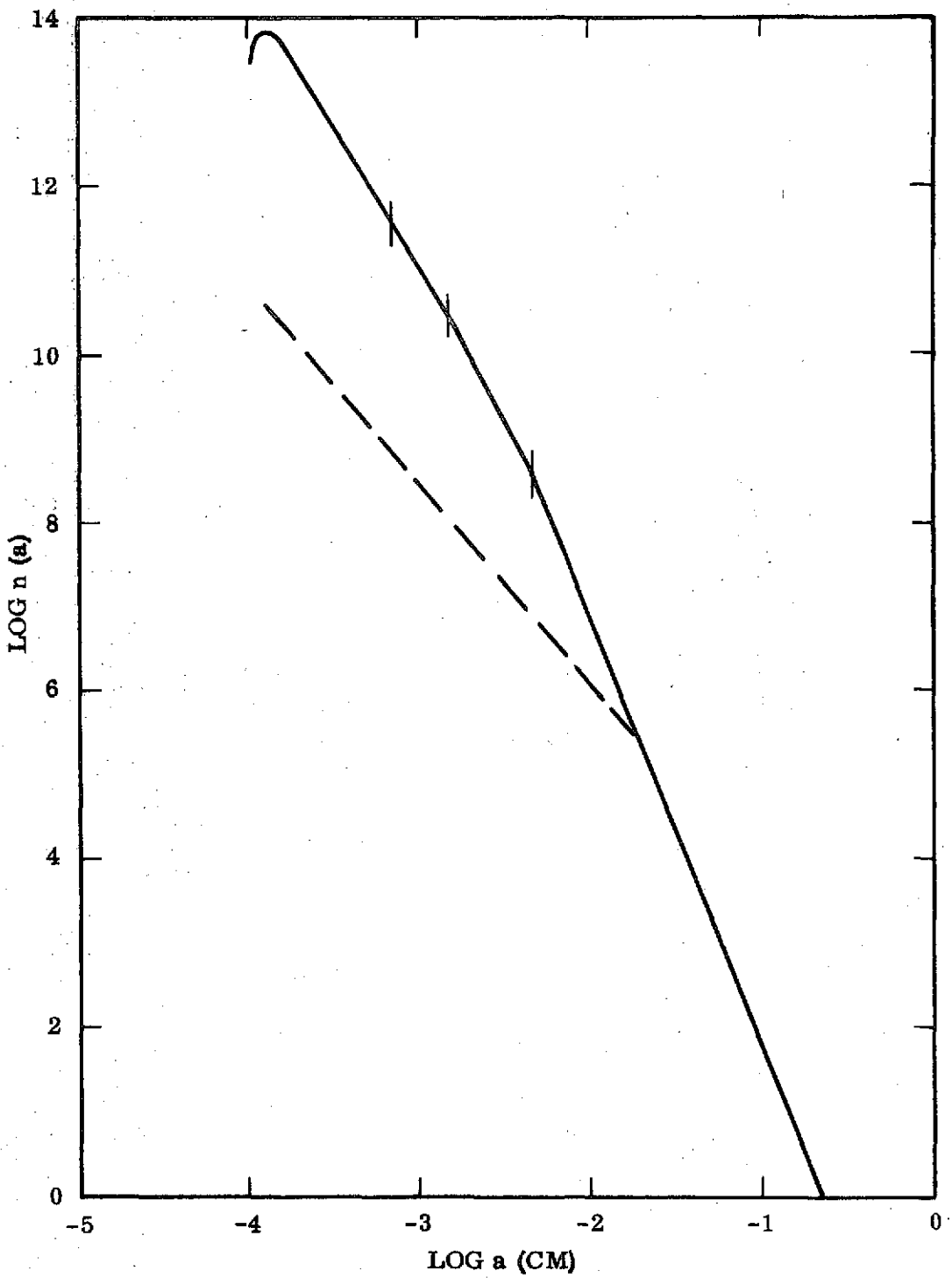

Figure 1 Particle size distribution.

small particles would make only a small contribution to the total scattered light.

It is of interest to compare our distribution to one derived by Taylor et al. (1973) in a similar manner. This is done in Fig. 2. The disparities arise from the different densities and size cutoffs used.

2. Production Rate

As discussed above, non-gravitational acceleration of Comet Encke implies a loss of $\sim 10^{13}$ g per orbital revolution. It is not known how much of this is in the form of dust, but Whipple (1967) suggests that the abundance of Taurid meteors is evidence that perhaps an old comet such as Encke releases a larger fraction of material in dust than does a "new" comet (see also Delsemme's 1973 review). Whipple (1967) goes on to estimate that, averaged over one period, Comet Enke contributes as much as 3.5×10^{6} g sec^{-1} of meteoritic material to the interplanetary cloud. If true, this would imply a much smaller degree of anisotropy of ejection than has been determined for this comet (Marsden and Sekanina, 1971, p. 1143). The distribution of particle sizes might differ from that for "new" comets, having fewer small particles.

We conservatively assume that the total mass lost per orbit is 10^{13} g, of which 10 percent is dust. This gives a simple average mass-loss rate of $dM/dt \simeq 9.6 \times 10^{3}$ g sec^{-1} as dust. As an approximation to the evaporation rate of water snow (Delsemme and Miller, 1971; Marsden, Sekanina and Yeomans, 1973), the mass-loss varies as r^{-2} for $r \leq r_c$ amd is zero at greater distances. The mass-loss rate at any particular heliocentric distance is then easily calculated; Table I gives the mass-loss at r = 0.8 AU for various assumed r_c.

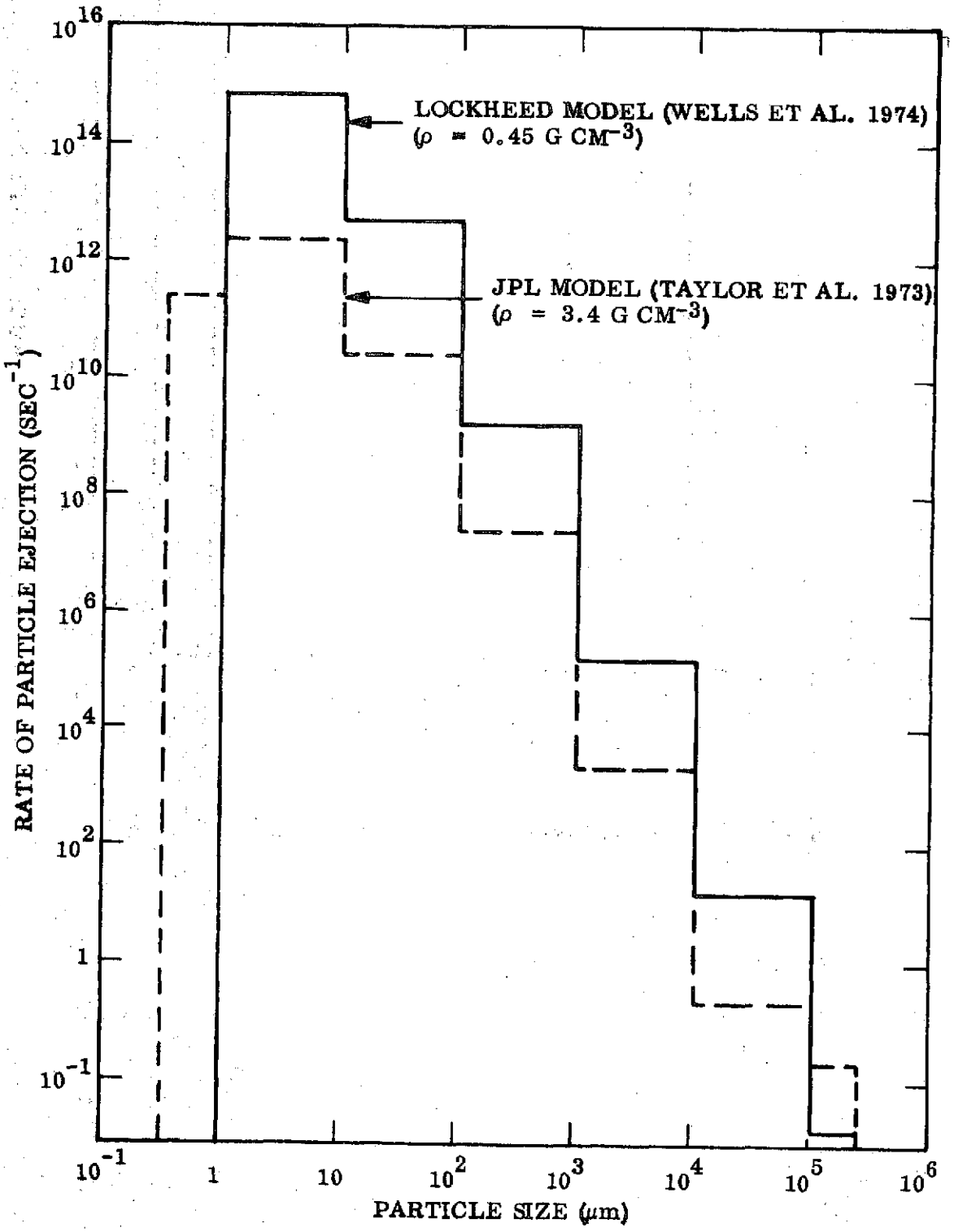

Figure 2 Comparison of distribution of particle sizes.

TABLE I. Dust Mass-Loss at 0.8 AU

r_c (AU)	dM/dt (10^4 g sec^{-1})
1.00	5.93
1.25	5.47
1.50	5.17
2.00	4.78
2.808	4.42

Thus, for this simple approximation, the mass-loss rate is not sensitive to the value of r_c, and $dM/dt \simeq 5 \times 10^4$ g sec^{-1} is a typical value for r = 0.8 AU.

3. Velocity Distribution

The evaporation of cometary ices (primarily H_2O) produces a flow from the nucleus which accelerates dust particles to their terminal ejection velocities within $\sim$ 10 nuclear radii (Probstein, 1968; Delsemme and Miller, 1971). Delsemme and Miller (1971) calculate the largest particle which the expanding vapor can lift against gravity; for ρ = 0.45 g cm^{-3}, R_n = 1.7 km and ρ_n = 1 g cm^{-3} we have

$$a_{max} \simeq 3.14 \times 10^{-17} Z \text{ cm}$$

where the rate of evaporation, Z (molecule $cm^{-2} sec^{-1}$), depends on heliocentric distance. In Figure 3 we show the velocity distribution from Delsemme and Miller (1971) expressed in terms of a/a_{max}. Using the evaporation rate as reported by Marsden, Sekanina and Yeomans (1973), at 0.8 AU $Z \simeq 4.9 \times 10^{17}$

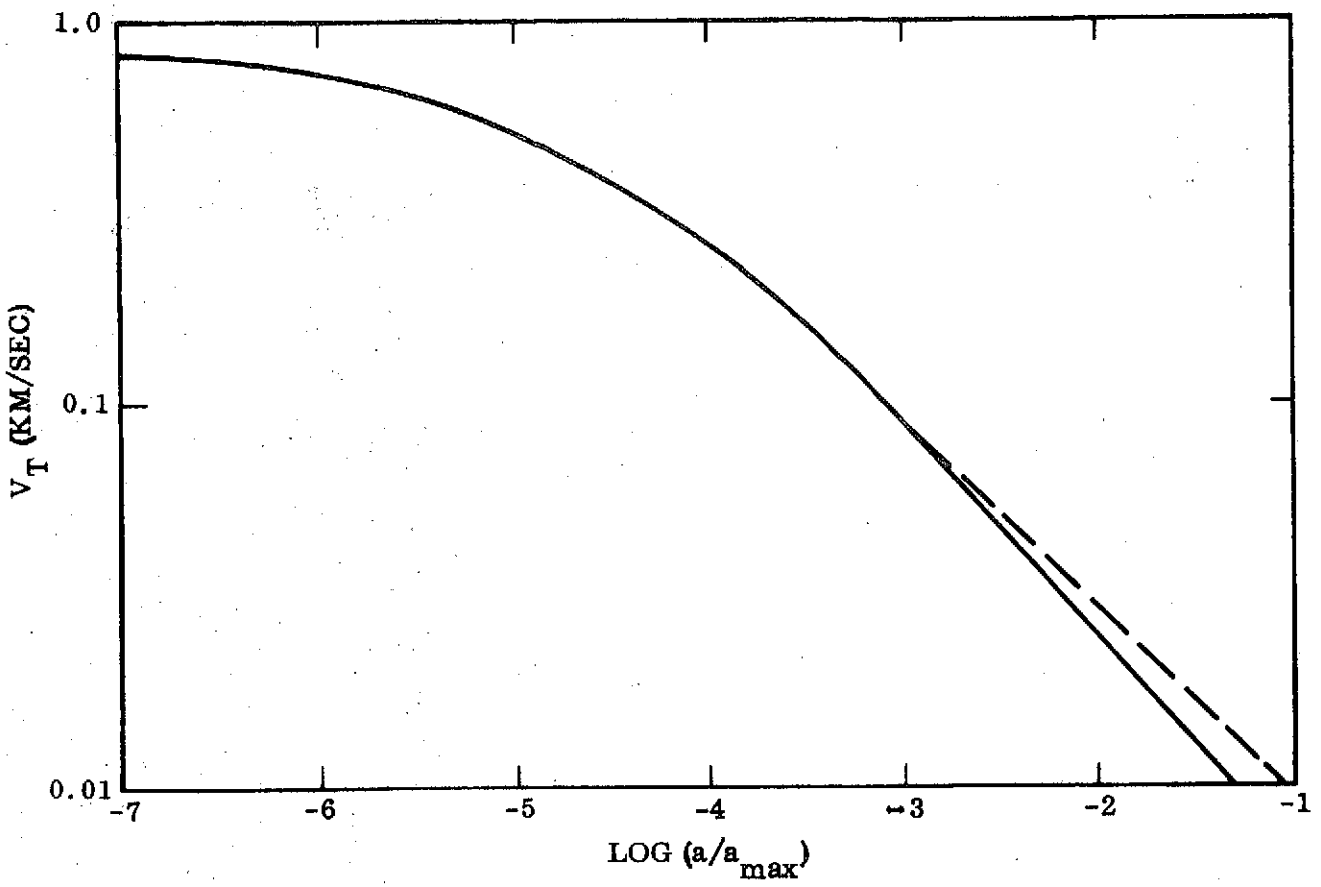

Figure 3 Terminal velocities of non-volatile particles.

and $a_{max} \simeq 15.5$ cm. Since Z varies roughly as r^{-2}, larger particles can be ejected at $r < 0.8$ AU. Also, as can be seen in Figure 3, at smaller heliocentric distances all particles tend to have nearly the same terminal velocity, while at larger distances $v \sim a^{-1/2}$ (approximately). If, as is likely, Comet Enke is not covered with ices, then the effective Z(r) should be reduced, thereby also reducing a_{max} and v(a).

For calculating sunlight scattering from dust, we divide the particle size distribution into six ranges and assign appropriate mean radii to each range. The root-mean-square, $(< a^2 >)^{1/2}$, is used to calculate the scattering by each size range. While $(< a^{1/2} >)^2$ is used for determining the terminal velocity, the result is not sensitive to the particular kind of averaging which is used because the velocity is a slowly-varying function of particle radius. The size ranges and derived properties are given in Table II, with $dM/dt = 5 \times 10^4$ g sec^{-1} and $a_{max} = 15.5$ cm as is appropriate for a heliocentric distance of 0.8 AU.

TABLE II. Particle Sizes and Terminal Velocities (0.8 AU)

Range (μm)	Production Rate (sec^{-1})	$(< a^2 >)^{1/2}$ (μm)	Geometric Scattering Contribution(%)	v (km sec^{-1})
1 - 1.5	1.51×10^{14}	1.28	9.8	0.53
1.5- 3	1.79×10^{14}	2.04	29.4	0.49
3 - 6.7	3.68×10^{13}	4.10	24.5	0.41
6.7- 14.4	5.03×10^{12}	9.35	17.4	0.33
14.4-44.4	8.77×10^{11}	20.9	15.2	0.25
44.4-a_{max}	2.34×10^{10}	62.9	3.65	0.15

The first five size ranges used in the Mie scattering code are discussed below; the final group contains particles sufficiently large that the geometrical approximation is adequate ("debris"). The scattering contribution (column 4) represents the relative total geometric cross section of each size range.

Because the particles attain their terminal velocities very near the cometary nucleus, throughout the coma (where they will be observed) their spatial distribution is given by

$$n_i(R) = \frac{P_i}{4\pi R^2 v_i} \quad cm^{-3}$$

where P_i is the production rate and v_i the terminal velocity for particles in the i^{th} size range; R is the radial distance from the nucleus.

This model shares with all current theoretical models the lack of asymmetry in ejection which must be present in order to produce the observed non-gravitational forces. The size distribution of dust particles has the virtue of being related to observations of actual comets, although there has been no analysis of an old comet (such as Encke) using the procedures described by Finson and Probstein (1968). Perhaps the lower curve in Figure 1, giving Whipple's (1968) distribution of interplanetary particles, would be a better representation for Comet Encke or the compilation by Dohnanyi (1972). The distribution used here contains a larger fraction of small particles ($1 < a < 5$ μm) which are relatively efficient scatterers, so our results may represent an upper limit to the sunlight scattering for a given dM/dt.

IV. TRAJECTORY

Comet Encke is a periodic comet with a period of 3.3 years. It shows greatly reduced activity after perihelion relative to before, and shows very little continuum radiation at any time, indicating a low dust content (Taylor et al., 1973). Encke never shows a type II (dust) tail and in some apparitions has shown no tail at all. The observations from 1885-1951 indicate that Encke's coma becomes observable at about 1.5 AU at the same time as the first appearance of its tail (Vsekhsvyatskii, 1964). The orbital characteristics of comet Encke are given in Table

TABLE III. Orbital Elements of Comet Encke

Orbital period (year)	3.30
Aphelion distance (AU)	4.09
Perihelion distance (AU)	0.34
Orbital inclination (deg)	12.4
Velocity at 1 AU (km s^{-1})	37.1
Velocity at perihelion (km s^{-1})	69.9
Orbital eccentricity	0.847

Vsekhsvyatskii (1964) has estimated a nominal value of 10^5 km for the diameter of Encke's coma reduced to a Sun-comet distance of 1 AU. Observational data on tail length are given by Yoemans (1973) and TRW (1972).

Many different kinds of missions to Encke have been proposed including fast and slow flybys. They do have certain elements in common. A nominal miss distance is about 10^2-10^3 km. One proposed probe trajectory calls for a rendevous at a heliocentric distance of about R_s= 0.8 AU. We have chosen this distance to calculate the absolute and relative luminosities of the dust, debris, and nucleus.

V. MIE SCATTERING

In this section the computer code used to calculate the Mie scattering of sunlight from the cometary dust is described. Results are then presented for scattering of dust particles in the coma of Comet Encke.

A. Mie Theory and Computer Code

Particulate radiation effects in particulate clouds can be calculated provided that the optical constant of the radiating particles are known. Gal and Kirch (1973 and Gal, 1974) reported a new computer code called GMIE to calculate scattering cross sections of interest. Calculations are based on MIE theory for a specified particulate column with a given complex index for refraction, range of wavelength, temperature, and particle sizes.

It should be noted that the GMIE code can be used to obtain scattering cross sections or differential cross section for any given spherical particle or particulate column with a given size distribution and index of refraction.

1. Electromagnetic Radiation Scattered by Absorbing Sphere

The passage of electromagnetic radiation through a particle cloud is generally accompanied by removal of a fraction of the energy from the incident beam. This fraction may be partly absorbed within the particles and partly scattered -- i.e., reappear in the same direction as well as in other directions. The characteristics of the scattered radiation are determined by the wavelength λ of the incident radiation, the refractive index ($m = n_1 - in_2$) of the particles and size as well as the shape of the discrete particles in the medium. For the radiation studies, we assume spherical particles with radius r.

The interaction of an electromagnetic wave with an absorbing sphere is described by the MIE theory (Fig. 4) and is discussed in detail elsewhere (van de Hulst, 1957). Classical MIE theory gives the intensity $I(W/cm^2)$ at a distance R and angle θ of the radiation scattered from a single spherical particle of radius r exposed to parallel monochromatic radiation of intensity I_o:

$$\frac{I}{I_o} = \frac{S(\theta)}{2(2\pi/\lambda)^2 R^2} \qquad (1)$$

where $S(\theta)$ is the scattering function per unit particle.

A computational scheme and computer code were provided by J. Dave of IBM (1968). These are based on the Ricatti-Bessel functions and give the MIE scattering cross section of absorbing spherical particles.

Computations are valid for all values of size parameters that occur in the theory regardless of whether they are large or small. The index of refraction of the particles are given in terms of their real and imaginary parts.

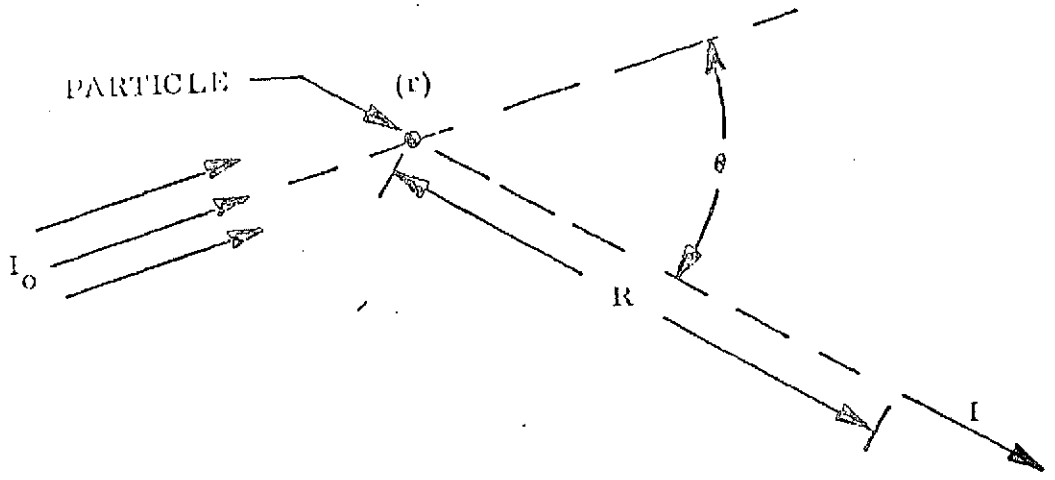

Fig. 4 Definition of Single-Particle Scattering

The extinction and scattering cross section are calculated from various combinations of the sum and products of the coefficients a_n and b_n. The usual expressions for a_n and b_n are:

$$a_n = \frac{\psi'_n(y)\,\psi_n(x) - m\,\psi_n(y)\,\psi'_n(x)}{\psi'_n(y)\,\xi_n(x) - m\,\psi_n(y)\,\xi'_n(x)} \tag{2}$$

$$b_n = \frac{m\,\psi'_n(y)\,\psi_n(x) - \psi_n(y)\,\psi'_n(x)}{m\,\psi'_n(y)\,\xi_n(x) - \psi_n(y)\,\xi'_n(x)} \tag{3}$$

where

m = the complex index of refraction

n = a positive integer

ψ and ξ = the Ricatti-Bessel functions defined by

$$\psi_n(z) = \left(\frac{1}{2}\,\pi\,z\right)^{1/2} J_{n+1/2}(z) \tag{4}$$

$$\xi(z) = \left(\frac{1}{2}\,\pi\,z\right) H^{(2)}_{n+1/2}(z) \tag{5}$$

with $J_{n+1/2}$ and $H^{(2)}_{n+1/2}$ the Bessel functions of first and third types. The prime denotes differentiation with respect to the argument of the function and

$$x = 2\pi\,r/\lambda \tag{6}$$

$$y = mx \tag{7}$$

where r is the particle radius and λ is the wavelength.

Once these scattering coefficients are defined, then extinction and scattering normalized cross section can be calculated with the following equations:

$$Q_{EXT} = \frac{2}{x^2} \sum_{n=1}^{\infty} (2n + 1)\,\text{Real}\,(a_n + b_n) \tag{8}$$

$$Q_{SCATT} = \frac{2}{x^2} \sum_{n=1}^{\infty} (2n + 1) \left(|a_n|^2 + |b_n|^2 \right)$$

Scattering efficiency (i.e., normalized scattering cross section) given by Eq. (9) can also be written as a function of scattering angle and the intensity in that direction:

$$Q_{SCATT} = \frac{1}{x^2} \int_0^{\pi} \left[i_1(\theta) + i_2(\theta) \right] \sin\theta \, d\theta \tag{10}$$

where

$$i_1(\theta) = |S_1(\theta)|^2$$

$$i_2(\theta) = |S_2(\theta)|^2$$

and

$$i_1(\theta) + i_2(\theta) = S(\theta) \tag{11}$$

$i_1(\theta)$ and $i_2(\theta)$ refer, respectively, to the intensity of light polarized perpendicularly and parallel to the plane through the direction of propagation of the incident and scattered beam. These intensities are given in terms of the complex amplitude functions $S_1(\theta)$ and $S_2(\theta)$:

$$S_1(\theta) = \sum_{n=1}^{\infty} \frac{2n + 1}{n(n + 1)} \left[a_n \pi_n(\cos\theta) + b_n \tau_n(\cos\theta) \right] \tag{12}$$

and

$$S_2(\theta) = \sum_{n=1}^{\infty} \frac{2n + 1}{n(n + 1)} \left[b_n \pi_n(\cos\theta) + a_n \tau_n(\cos\theta) \right] \tag{13}$$

The phase functions π_n and τ_n appearing in Eqs. (12) and (13) can be expressed in terms of the Legendre polynomials, P_n, as follows:

$$\pi_n(\cos\theta) = \frac{d P_n(\cos\theta)}{d\cos\theta}$$

$$\tau_n(\cos\theta) = \cos\theta\, \pi_n(\cos\theta) - \sin^2\theta \frac{d\pi_n(\cos\theta)}{d\cos\theta} \tag{14}$$

The detailed computational method to obtain these Legendre polynomials with recurrence relationships is discussed elsewhere (Dave, 1968).

If there is no absorption, i.e., $n_2 = 0$, then $Q_{EXT} = Q_{SCATT}$. Otherwise, Q_{ABS}, the efficiency factor for absorption, is given by

$$Q_{ABS} = Q_{EXT} - Q_{SCATT} \tag{15}$$

Equation (9) or (10) gives the total scattered intensity. On the other hand, one may need to know the fraction of energy scattered into the forward and backward directions. This is obtained in terms of normalized cross section given in Eqs. (16) and (17), respectively

$$Q_{TRANS} = \frac{1}{x^2} \int_0^{\pi/2} \left[i_1(\theta) + i_2(\theta) \right] \sin\theta\, d\theta \tag{16}$$

and

$$Q_{REF} = \frac{1}{x^2} \int_{\pi/2}^{\pi} \left[i_1(\theta) + i_2(\theta) \right] \sin\theta\, d\theta \tag{17}$$

2. Solar Scattering Cross Section for a Spherical Particle

With the help of the basic MIE scattering theory, particular scattering due to sunshine will be treated through an equivalent normalized differential solar-scattering cross section. The sun is approximately half a degree as observed

from the earth, and calculations similar to those derived by Gal and Kirch (1973) for earthshine scattering would require evaluation of scattering function $S(\theta)$ for smaller than 1 deg, which is our present minimum step size. Approximate differential cross section will be obtained by averaging the basic MIE scattering function over a small angular increment ($\Delta\theta$) to account for the finite solar disk.

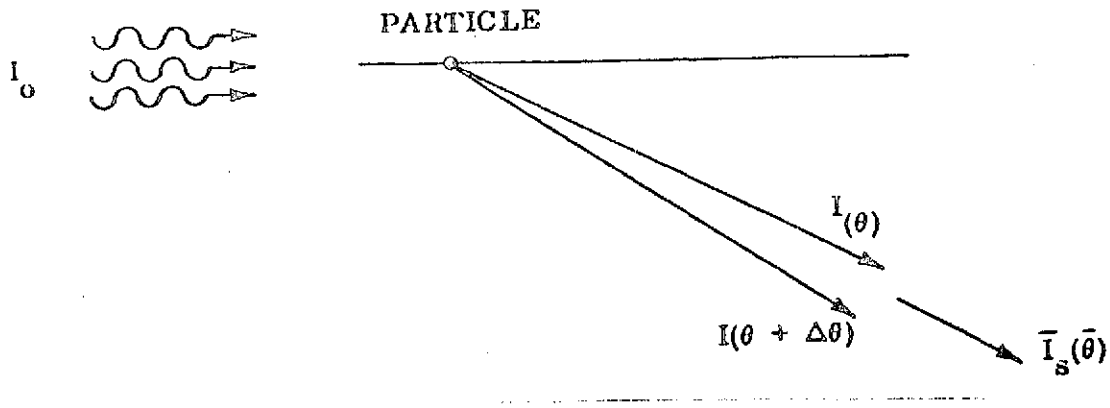

Fig. 5 Solar Scattering Model

From Eq. (1)

$$\frac{\left(I_S R^2\right)}{I_o} = \frac{1}{2\left(\frac{2\pi}{\lambda}\right)^2} \bar{S}(\theta) \tag{18}$$

The normalized differential cross section can be obtained by dividing Eq. (18) with the geometrical cross section $G = r^2 \pi$

$$(dQ) = \left(\frac{I_S R^2}{\pi r^2 I_o}\right) = \frac{1}{2\pi\left(\frac{2\pi r}{\lambda}\right)^2} \bar{S}(\theta) \qquad (sr^{-1}) \tag{19}$$

Equation (19) yields the normalized scattering cross section for a single spherical particle.

3. Column Average Cross Section and Radiance

a. Column Scattering

The extension to the case of scattering from a column of particles is straightforward upon adopting restrictive assumptions. First, the distance R must be large compared to the column dimensions so that scattering angle is essentially

constant for a given I_o direction. Also, the column must be optically thin. This requirement means that: (1) each particle is exposed to the incident intensity I_o, regardless of location; and (2) the radiation scattered from one particle does not interact with others as it passes from the column; i.e., there is no multiple scattering.

These assumptions allow the scattered intensities to be added. With the help of Eq. (19) we can define a cloud averaged differential cross section, $\bar{\sigma}$.

$$\bar{\sigma} = \sum_i (dQ)_i \; r_i^2 \; \pi \, (N_i/N_t) \quad (\mu m^2 \; sr^{-1}) \tag{20}$$

where

N_t = the total number of particles
N_i = the number i^{th} particles
r_i = the radius of the i^{th} particle

b. Column Radiance

Figure 6 shows the geometry; the solid angle of the instrument is given by $\Omega = A/L$, and the scattering cloud volume is $V = A\ell$, where A is the column surface area, and ℓ is the depth of the column. The total number of particles in the scattering values is

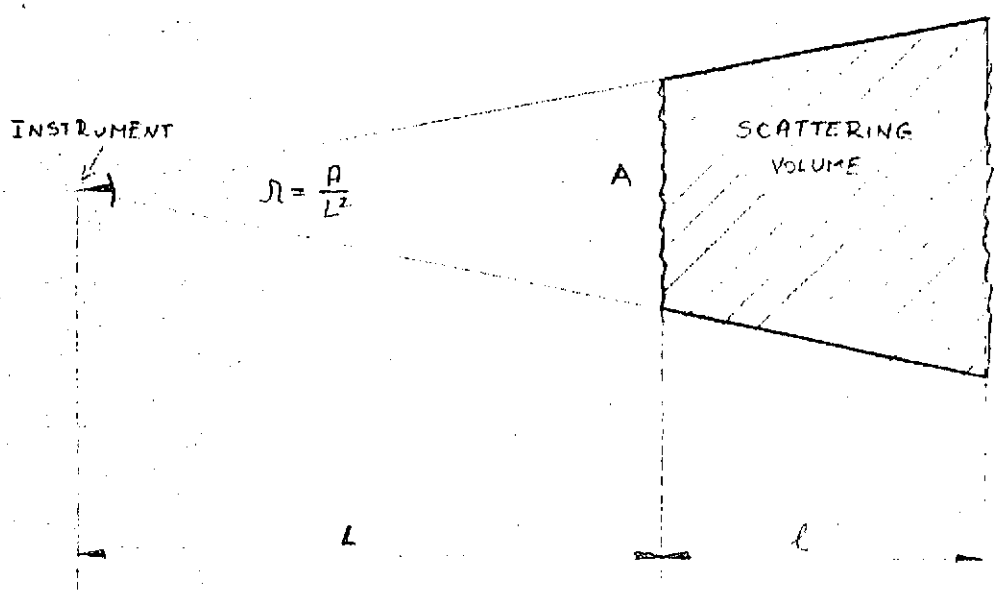

Figure 6 Definition of Scattering Values

$N_t = n A \ell$, where n is the particle density. The incident intensity $I_{o\lambda}$(watt/cm^2, μ) can be calculated assuming the sun as a blackbody at a temperature $T_{sun} = 6000°K$, and sun is approximately half a degree as observed from the earth

$$I_{o\lambda} = B_\lambda (T = 6000) \quad (\Delta\alpha) \quad (W\ cm^{-2} \mu m^{-1}) \tag{21}$$

where

$$B_\lambda = \frac{1.19 \quad 10^4 \ (1/\lambda)^5}{\exp\left(\frac{1.4384 \times 10^4}{\lambda\ T_s}\right) - 1} \qquad (W\ cm^{-2} sr^{-1} \mu m^{-1}) \tag{22}$$

where λ is the wavelength in microns, and $(\Delta\alpha)$ is solid angle of the sun viewed from the column ($6.8\ 10^{-5}$ sr) at 1 AU.

The column radiance is defined as

$$N_\lambda = \frac{J_\lambda}{A} \qquad (W\ cm^{-2}\ sr^{-1} \mu m^{-1}) \tag{23}$$

Substituting Eqs. (19 through (22) into Eq. (23), we obtain

$$N_\lambda = B_\lambda\ n_T\ l\ (\Delta\alpha) \sum_{i=1}^{5} (dQ)_i\ r_i^2 \pi \quad (N_i/N_t) \quad (W\ cm^{-2} sr^{-1} \mu m^{-1}) \tag{24}$$

Equation (24) has been programmed into our GMIE code; additional inputs required are particle size, its distribution, and the column depth, ℓ.

B. Mie Scattering From Cometary Dust Particles

We have inputed the comet Encke dust distribution into the GMIE code for various indices of refraction. The normalized scattering and absorption cross sections given in Eqs. (10) and (15) are plotted in Figure 7 for an index of refraction of 1.7-.05 i. Figure 8 shows a plot of the scattering function as a function of scattering angle for a dielectric particle of 0.65 μm radius with an index of refraction n = 1.7-.05 i. More plots of particle scattering functions are found in Appendix A showing the effect of particle sizes and indices of refraction. Also, the angular dependence of the polarization is plotted for a few select cases. To calculate the scattered sunlight from the comet, we chose an index of refraction of 1.7-.05 i to represent cometary dust particles which are probably primarily silicates containing metallic elements (Wickramasinghe and Krishna Swamy, 1968). Column densities are calculated in Appendix B. The results of the Mie scattering calculations are presented in Table IV where the wavelength dependence of the scattered radiance N_λ from Eq. (23) is presented as a function of the Sun-Comet-Probe angle. The functional dependence on wavelength and angle of the average differential cross section $\bar{\sigma}$ from Eq. (20) is displayed graphically in Figs. 9 and 10 for a few selected cases. Figure 9 shows the effect of view angle on $\bar{\sigma}$ at $\lambda = 0.5$ μm. The minimum scattering at this wavelength can be seen to occur in the 0-90° region. The wavelength dependence of the scattered radiance is displayed in Figure 10 for several view angles. It would appear that the scattering in the 0-90° range is relatively insensitive to wavelength dependence.

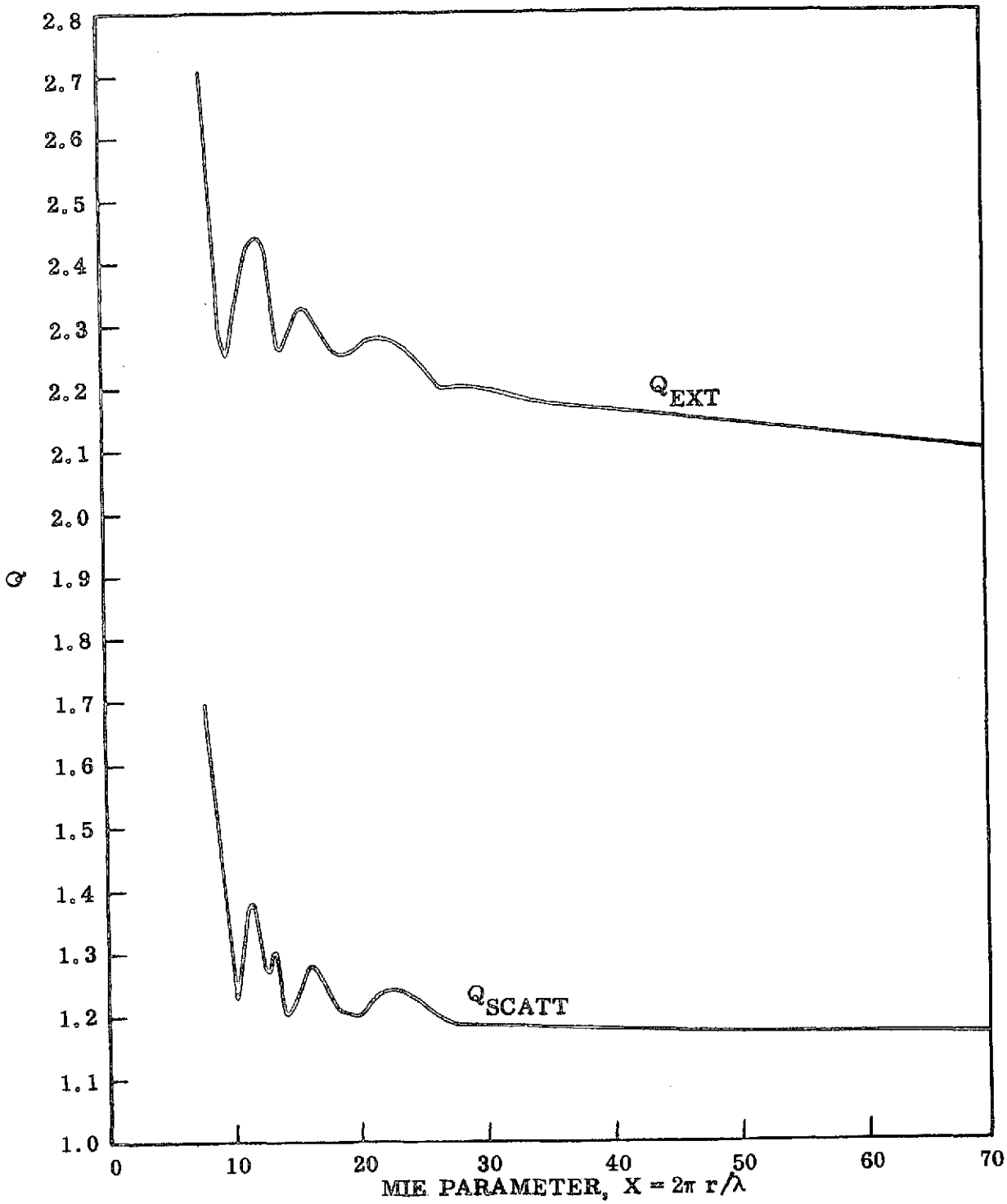

Figure 7 Scattering efficiency vs. Mie parameter for n=1.7-.05 i.

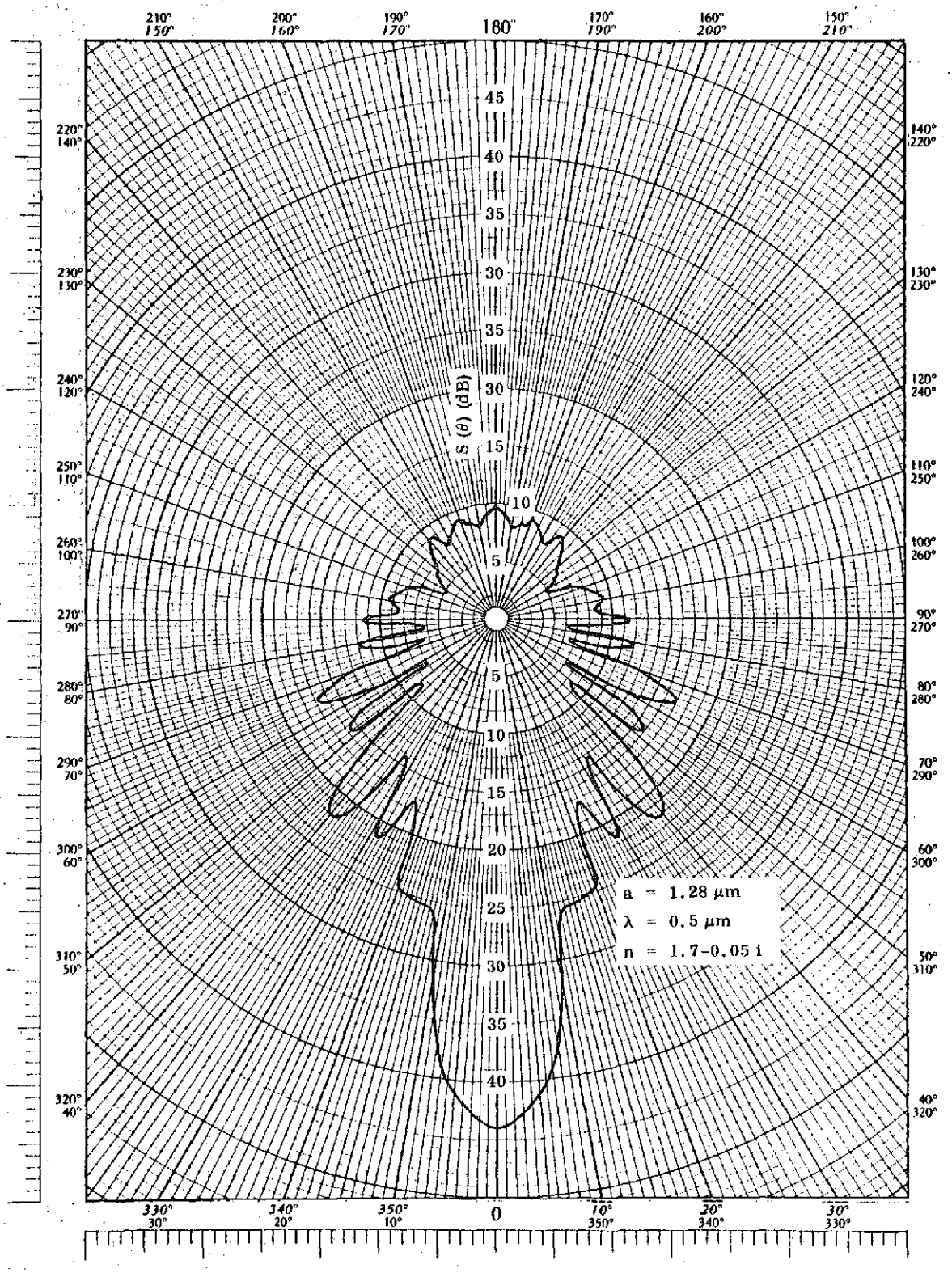

Figure 8 Angular dependence of scattering functions, a=1.28 μm, n=1.7-.05 i.

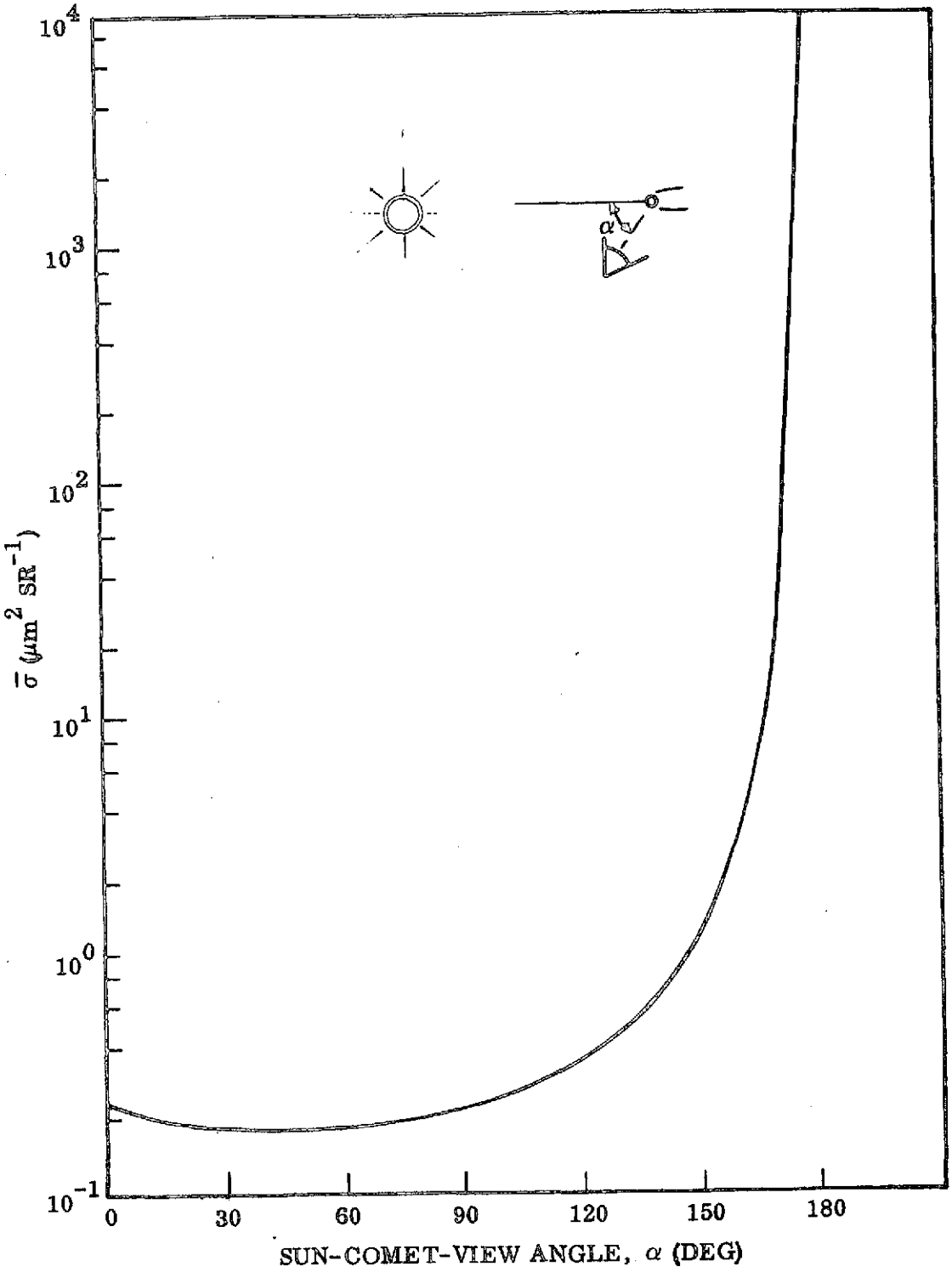

Figure 9 Angular dependence of average scattering cross section, $\lambda = 0.5$ μm

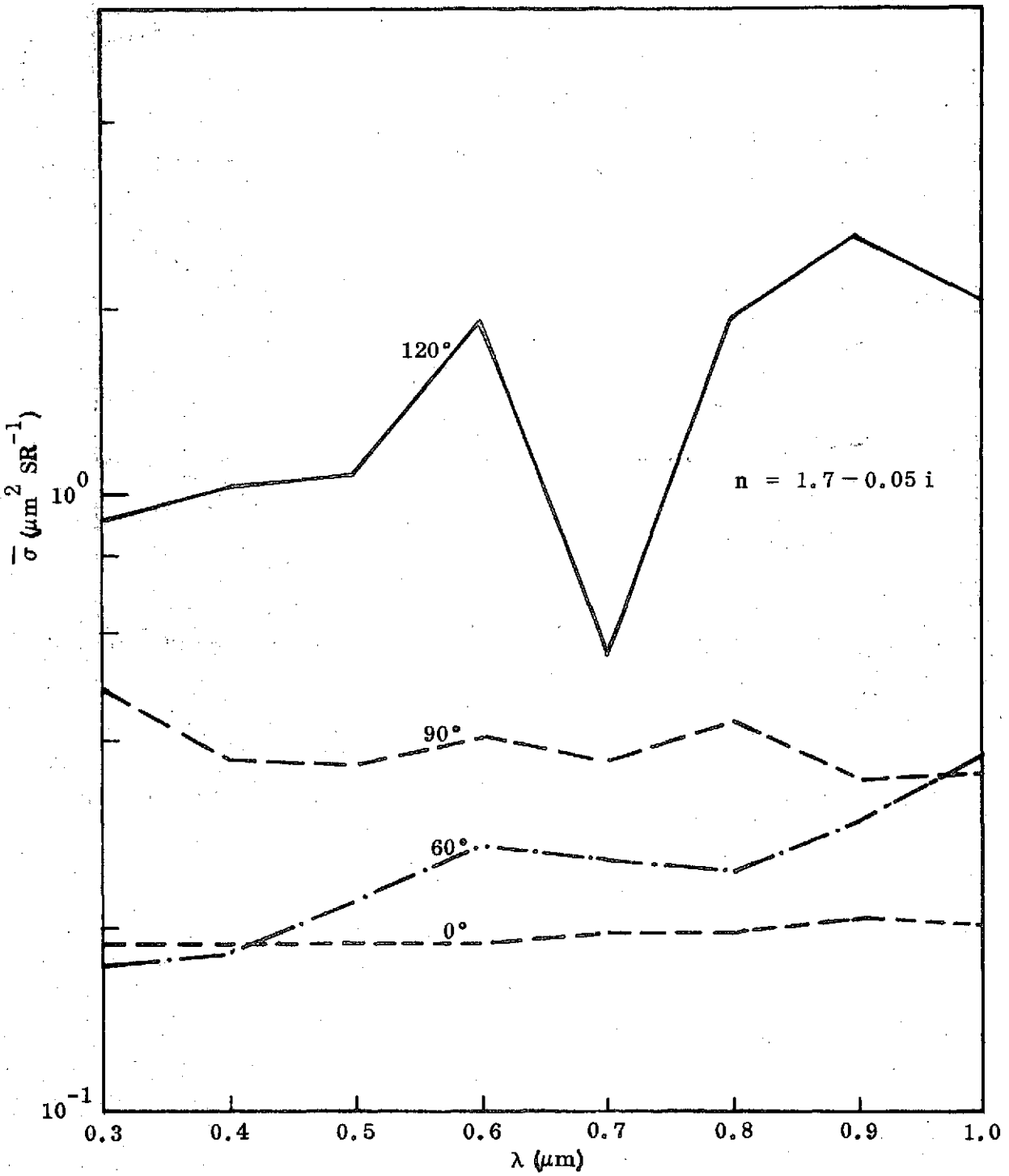

Figure 10 Wavelength dependence of average scattering cross section.

TABLE IV. Radiance of Comet Dust at R_s = 0.8 AU
N_λ(w $cm^{-2} sr^{-1} \mu m^{-1}$)

	Sun-Comet-Probe Angle						
	0°	30°	60°	90°	120°	150°	180°
0.3	2.7 -6)	2.4(-6)	2.3(-6)	2.2(-6)	6.2(-6)	1.2(-5)	1.4
0.4	4.8(-6)	4.2(-6)	4.1(-6)	4.1(-6)	8.3(-6)	2.3(-5)	1.5
λ 0.5	5.4(-6)	4.6(-6)	4.4(-6)	5.4(-6)	8.9(-6)	2.6(-5)	1.1
(μm)0.6	5.0(-6)	4.1(-6)	4.1(-6)	6.0(-6)	9.0(-6)	4.2(-5)	6.8(-1)
0.7	4.3(-6)	3.5(-6)	3.3(-6)	4.7(-6)	6.8(-6)	9.9(-6)	4.2(-1)
0.8	3.7(-6)	2.9(-6)	2.5(-6)	3.6(-6)	6.3(-6)	2.8(-5)	2.7(-1)
0.9	2.9(-6)	2.3(-6)	2.2(-6)	3.4(-6)	4.0(-6)	3.0(-5)	1.8(-1)
1.0	2.6(-6)	1.8(-6)	1.8(-6)	3.1(-6)	1.4(-6)	1.8(-5)	1.2(-1)

These results, which have been calculated for a heliocentric distance of R_s = 0.8 AU, can be approximately scaled to other distances by the law

$$N_\lambda(R_s) = N_\lambda\ (0.8)\ \left(\frac{0.8}{R_s}\right)^{4-\zeta}, \qquad (25)$$

where ζ accounts for the terminal velocity dependence on heliocentric distance and R_s is in AU. Equation (25) reflects the inverse square dependencies of the solar irradiance and dust production rates. The heliocentric dependence of the terminal velocities arises primarily in the case of Encke from the fact that the acceleration of the dust particles is dependent on the number of collisions the particles undergo with effusing gas molecules. Hence,

the terminal velocities depend on particle sizes and the vaporization rate of gas from the nucleus. In the case of Encke dependence on the temperature of the nucleus is of lesser importance. For the particle sizes of importance here the heliocentric dependence can be approximated by setting $\zeta = 0.4$. This law will hold for R_s out to about 1.5 AU where the dust production ceases due to the threshold effect of ice evaporation.

VI. SCATTERING BY DEBRIS PARTICLES

For particles in the 10^{-2}-10 cm range, scattering can be treated essentially as isotropic with a geometrical cross section. Thus, the differential cross section can be written as

$$\frac{d\sigma}{d\Omega} = \frac{\pi a^2 a_n}{4\pi}, \tag{26}$$

where the albedo a_n is taken equal to that of the nucleus, 0.1. Calculating an average differential cross section for $R_s = 0.8$ AU using the distribution in Table II results in

$$\frac{d\sigma}{d\Omega} = \frac{\bar{a}^2 a_n}{4} = 9.9 \times 10^{1} \ \mu m^2 sr^{-1} \tag{27}$$

where $\bar{a}^2$ is the rms radius of large particles, $a > 44$ μm. The column density for the debris particles is given by Eq. (B-3) which results in

$$n_T = \frac{P_i}{v_i} \frac{1}{4\pi R_{min}} = 2.5 \times 10^{-1} \text{ particles cm}^{-2}. \tag{28}$$

Using Eqs. (27), (28) with Eq. (24), we then would get a scattered brightness for large particles at $R_s = 0.8$ AU for $\lambda = 0.5$ μm of

$$N_\lambda = 8.9 \times 10^{-8} \text{ W cm}^{-2} sr^{-1} \mu m^{-1}. \tag{29}$$

As can be seen from Table IV, this contribution is less than the small particle Mie scattering by a factor of 50. So it can be concluded, followin our model, that the small size dust particles contribute much more to the scattered brightness than the large size debris particles.

VII. SCATTERING BY ICE PARTICLES

It is difficult to precisely assess the ice particle distribution and production rates for Encke. We shall assume here that the ice particles can be represented by particles with a radius of 300 μm (Delsemme and Miller, 1971). An upper limit for the ice production rate can be derived from the OGO-5 satellite observations of Lyman-α emission from Encke. The observed emission corresponded to a production rate of $Q(H) = 5 \times 10^{26}$ atoms $sr^{-1}s^{-1}$ for hydrogen atoms at $R_s = 0.715$ AU (Bertaux et al., 1973). Assuming that all the H atoms came from ice particles results in a production rate for water $Q(H_2O) = 3 \times 10^{27}$ molecules s^{-1} (Delsemme and Rud, 1973). For icy grains of 300 μm radius, we then have $Q_{ice} \sim 2 \times 10^{9}\ s^{-1}$.

Using these numbers, it is possible to estimate the scattered sunlight assuming an albedo of 0.9. For the differential cross secti we have

$$\frac{d\sigma}{d\Omega} = 2.0 \times 10^{4}\ \mu m^{2}\ sr^{-1}, \tag{30}$$

and the column density would be

$$n_T \sim 9 \times 10^{-2} \quad \text{particles cm}^{-2}. \tag{31}$$

An estimate of the scattered light would then yield for $\lambda = 0.5$ μm and $R_s = 0.8$ AU

$$N_\lambda = 6 \times 10^{-5}\ W\ cm^{-2}\ sr^{-1}\ \mu m^{-1}. \tag{32}$$

This result is of the same order of magnitude as the results for Mie scattering for cometary dust suggesting that scattering by ice particles surrounding the nucleus could be a major contributer to scattered sunlight. On the otherhand, our ice model is tentative and ice production rates could be revised downward.

VIII. SUNLIGHT REFLECTION FROM THE NUCLEUS

We have assumed an albedo of 0.1 for the nucleus so the brightness of the nucleus following Eq. (24) is given by

$$N_\lambda^{nuc} = B_\lambda(\Delta\alpha) \frac{0.1}{2\pi} , \tag{33}$$

where $\Delta\alpha$ is the solid angle subtended by the sun at a given heliocentric distance, R_s. It varies as R_s^{-2}. It is assumed here that the scattering is isotropic into 2π sr. For $\lambda = 0.5$ μm and $R_s = 0.8$ AU, we have

$$N_\lambda^{nuc} = 5.7 \times 10^{-3} \text{ W cm}^{-2}\text{sr}^{-1}\mu\text{m}^{-1}. \tag{34}$$

IX. COMPARISON OF BRIGHTNESS OF NUCLEUS TO BACKGROUND BRIGHTNESS

The contribution to the background brightness from the comet dust is tabulated in Table V. Taking one specific case we can compare the brightnesses from the nucleus to the background brightness. For the case with a heliocentric distance of 0.8 AU, $\lambda = 0.5$ μm, and view angle, $\alpha = 90^\circ$, the radiance levels are presented in Table IV.

TABLE V. Radiances at $R_s = 0.8$ AU for $\lambda = 0.5$ μm, $\alpha = 90^\circ$

		Particulate Scattering		
	Nucleus	Dust	Debris	Ice
Radiances (W cm^{-2} sr^{-1} μm^{-1})	5.7×10^{-3}	5.4×10^{-6}	8.9×10^{-8}	6×10^{-6}

The background from particulate scattering is 2 to 3 orders of magnitude below the intensity from the nucleus. The relative particle to nuclear brightness levels in Table IV are expected to vary less than an order of magnitude going into perhelion (0.34 AU) or out to "turn on" at about 2 AU.

Based on these calculations there should be no difficulty in viewing the nucleus from masking by particulate scattering. The particles are optically thin and the brightness levels are several orders of magnitude down from that of the nucleus.

X. OPTIMIZATION OF IMAGING SYSTEM

In terms of scientific value, resolution as high as possible is desired to examine the nature and composition of the surface. One of the problems with high resolution imagery and perhaps the limiting one is the large relative velocity of the spacecraft and comet which can be of the order of 10 km/sec. This, of course, would depend on the particular mission trajectory selected. Blurring of the image while a pixel cell is being exposed necessitates short exposure times. This requirement would argue for a high sensitivity-low noise system such as an image disector or a spin-scan camera. As an example of some numbers consider the case where the desired resolution element is ten meters squared on the surface of the nucleus and the bandwidth is 0.1 μ. Then the photon rate corresponding to a resolution element would be $N = 1 \times 10^{21}$ photons-sec^{-1}-sr^{-1}. The solid angle subtended by a 5" diameter telescope at 1000 km would be about 2.5×10^{-15} ster and would result in photon rate at the detector of 3×10^{6} photons/sec per pixel cell. If the transverse velocity of the comet with respect to the spacecraft is of the order of 10 km/sec then exposure times/pixel of no more than 1 msec are required. This corresponds to 6×10^{3} photons/pixel which is sufficient to detect intensity variations from the surface of 4%. It should be noted that the intrinsic readout noise of a vidicon system corresponds to about 1000 electrons/pixel.

Other options which should be considered with an imaging system are use of polarizers to gain polarization information about the nuclear surface Because the illumination of the nucleus will be quasi-lambertian, viewing at different phase angles will afford information regarding surface irregularities. Shadow heights can be used to topographically map the surface. The use

of filters to block out line and band emission features in the bandwidth of the imaging system may be deemed wise.

It is concluded that dust and debris scattering will not compromise the nucleus imaging mission and that high relative velocities warrant the use of a low noise imaging system such as a spin-scan camera.

ACKNOWLEDGEMENTS

One of the authors (W.C.W.) would like to thank the following scientists for informative discussions regarding physical properties of Encke, Mie scattering and optimum imaging systems: B. Donn, R. Giese, J. Kumer, S. Mende, M. Mumma, W. Michel and Z. Sekanina.

REFERENCES

Bertaux, J.L., Blamont, J.E. and Festou, M.; "Interpretation of Hydrogen Lyman-Alpha Observations of Comets Bennett and Encke," Astron. and Astrophys., 25, 415, 1973.

Corben, H.C.; "Remarks on a Comet Probe," in Space AGE Astronomy, Academic Press, New York, 380-382, 1962.

Dave, J.V.; Subroutines for Computing the Parameters of the Electromagnetic Radiation Scattered by a Sphere, IBM Scientific Center, Palo Alto, Calif.,

Delsemme, A.H. and Miller, D.C.; "Physico-Chemical Phenomena in Comets-III. The Continuum of Comet Burnham (1960 II)," Planet. Space Sci., 19, 1229, 1971. 1229, 1971.

Delsemme, A.H. and Rud, D.A.; "Albedos and Cross-sections for the Nuclei of Comets 1969 IX, 1970 II, and 1971 I," Astron. and Astrophys., 28, 1, 1973.

Delsemme, A.H.; Space Sci. Rev., 15, 89. 1973.

Dohnanyi, J.S.; Icarus 17, 1, 1972.

Donn, B., Powell, R., and Remy-Battiau, L.; "Interpretation of the Continuous Spectra of Comets," Nature 213, 379, 1967.

Finson, M.J. and Probstein, R.R.; "A Theory of Dust Comets. II. Results for Comet Arend-Roland," Astrophys. J., 154, No. 1, Part 1, 353, 1968.

Friedlander, A.L.; On the Problem of Comet Orbit Determination for Spacecraft Intercept Missions, IIT Research Institute Rep. T-19, 1967 (N67-28832).

Gal, G.; Electromagnetic Scattering From Particulate Clouds, Technical Report, LMSC D401089, Contract N00030-74-C-01-00, April, 1974.

Gal, G. and Kirch, H.; Particulate Optical Properties in Rocket Plumes, Final Report, Contract F04611-72-C-0034, DARPA O/N 1857, AFRL-TR-73-99, LMSC D354502, November 1973.

Lust, R.;"Cometary Probes," Space Science Rev. 10, 217-229, 1969.

Lyttleton, R.A.; Astrophy. Space Sci., 15, 175, 1972.

Maines, P., Grudinska, S. and Stawiskowski, A.; "Observations Physiques de la Comete Periodique Giacobini-Zinner (1959b)," Annales d'Astrophysique, 23, 788-796, 1960.

Marsden, B.G. and Sekanina, Z.; Astron. J. 79, 413, 1974.

Marsden, B.G., Sekanina, Z. and Yeomans, D.K.; Astron. J. 78, 211, 1973.

Marsden, B.G. and Sekanina, Z.; Astron. J. 76, 1135, 1971.

Opik, E.J.; "The Stray Bodies in the Solar System, Part II," Adv. Astron. Astrophys. 4, 302, 1966.

Porter, J., Herrick, S., Rabe, E. and Roemer, E.; "Report on Comet Fly-by," European Space Res. Org. Rep. ESRO No. CFSG/10, 28.6, 1965.

Probstein, R.F.; Problems in Hydrodynamics and Continuum Mechanics, Soc. Indust. Applied Mech., Philadelphia, Pa., 568, 1958.

Roemer, E.; Mercury 1, No. 6, 18, 1972.

Roemer, E.; "Comet Notes," Mercury 1, 18-19, 1972.

Roemer, E., "The Dimensions of Cometary Nuclei," Mem. Soc. Roy. des Sci. de Liege, 12, 23, 1966.

Sekanina, Z.; private communication, 1974.

Sekanina, Z. and Miller, P.D.; "Comet Bennett 1970 II," Science 179, 565-567, 1973.

Sekanina, Z.; "Dynamical and Evolutionary Aspects of Gradual Deactivation of Short-Period Comets," Astron. J. 74, No. 10, 1223, 1970.

Sekanina, Z.; "Total Gas Concentration in Atmospheres of the Short Period Comets and Impulsive Forces Upon Their Nuclei," Astron. J. 74, 944-950, 1969.

Sekanina, Z.; Astron. J. 74, 1223, 1969b.

Sekanina, Z.; Astron. J. 74, 944, 1969a.

Swings, P.; "Objectives of Space Investigations of Comets," in Space Age Astronomy, Academic Press, New York, 370-379, 1962.

Taylor, F.W., Michaux, C.M. and Newburn, R.L., Jr.; A Model of the Physical Properties of Comet Encke, JPL Technical Report 32-1590, NASA-CR-135707, Oct. 1973.

TRW, Study of a Comet Rendevous Mission, TRW Tech. Rep. 72-87, 1972.

van de Hulst, H.C.; Light Scattering by Small Particles, New York, Wiley, 1957.

Verniani, F.; Space Sci. Rev. 10, 230, 1969.

Verniani, F.; J. Geophys. Res. 78, 8429, 1973.

Vsekhsvyatskii, S.; Physical Characteristics of Comets, NASA TT F-80, 1964.

Whipple, F.L.; Smithsonian Astrophysical Observatory Special Report 239, 1967.

Whipple, F.L.; in IAU Symposium No. 33, p. 481, 1968.

Whipple, F.L. and Douglas-Hamilton, D.H.; "Brightness Changes in Periodic Comets," Mem. Soc. Roy. des. Sci. de Liege 12, 469-480, 1965.

Whipple, F.L.; "Solid Particles in the Solar System," J. Geophys. Res. 64, 1653-1664, 1959.

Whipple, F.L.; "A Comet Model. 1. The Acceleration of Comet Encke," Astrophys. J. 111, 375-394, 1950.

Wickramasinghe, N.C. and Krishna Swamy, K.S.; Astrophys. J. 154, 397, 1968.

Yoemans, D.; Physical Description and Recovery Data for P/Encke, Computer Sciences Corp., Silver Springs, Md., 1973.

APPENDIX A

ANGULAR DISTRIBUTIONS FOR SINGLE PARTICLE MIE SCATTERING

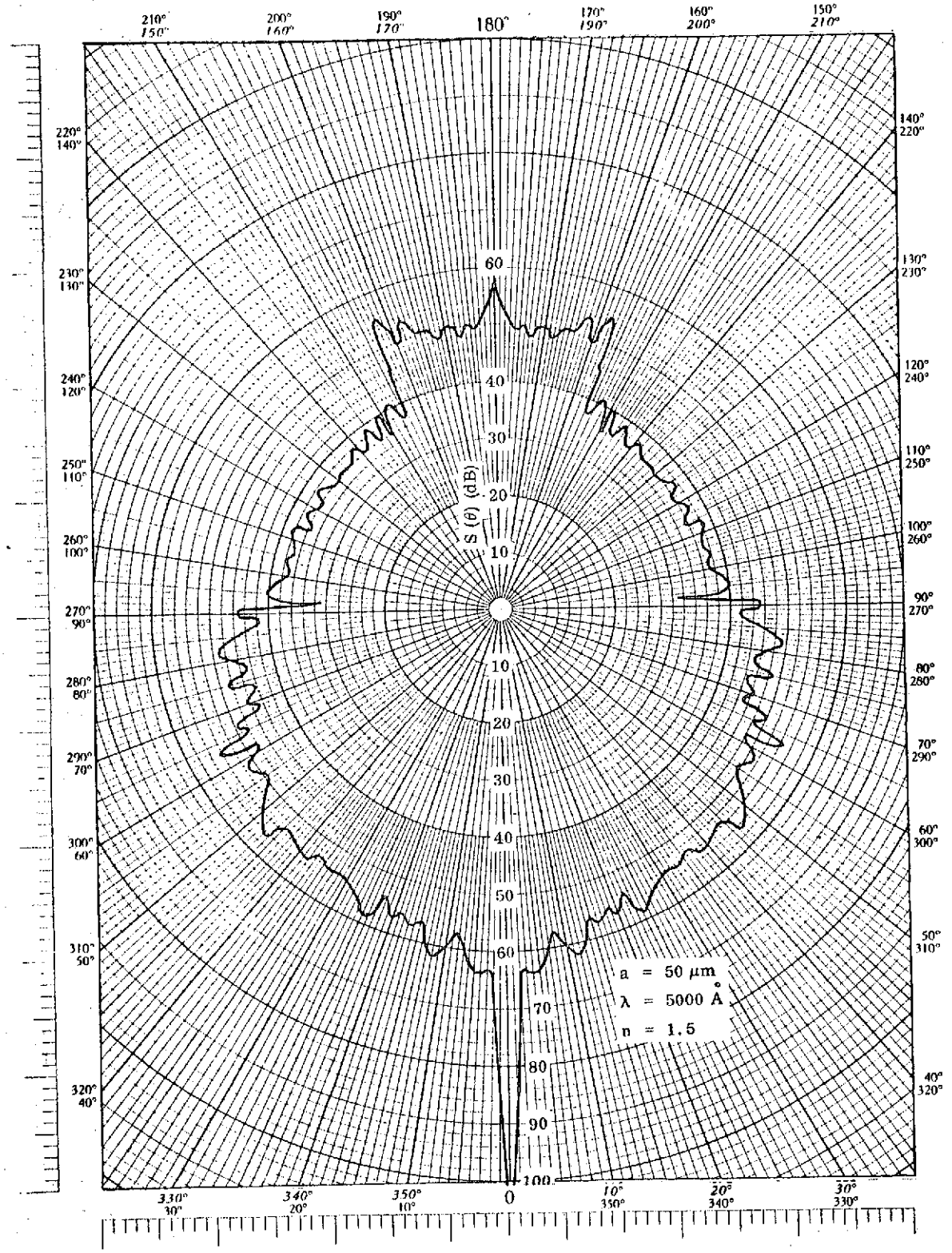

Figure A1 Angular dependence of scattering function, a=50 μm, n=1.5.

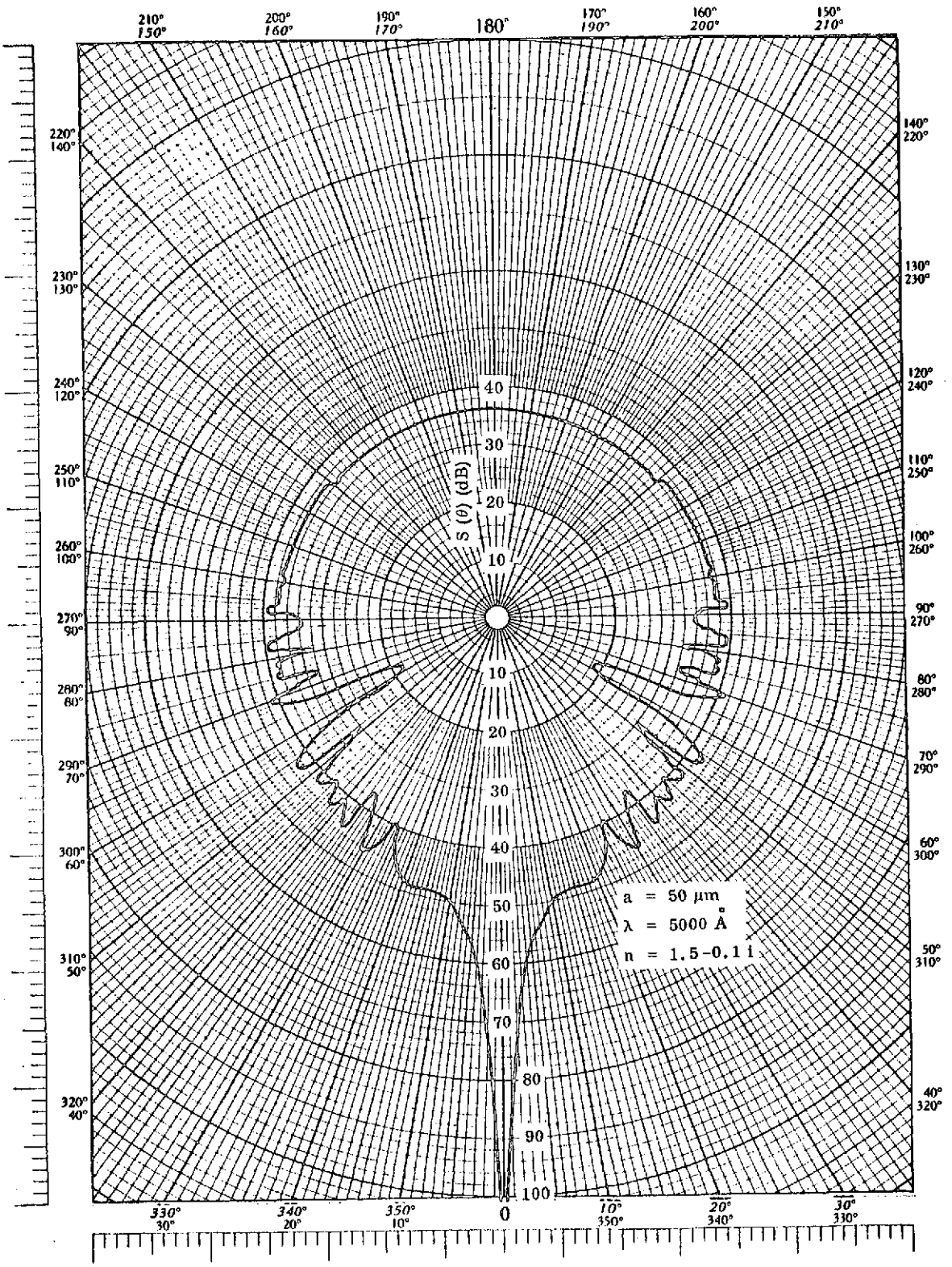

Figure A2 Angular dependence of scattering function, a=50 μm, n=1.5-.1 i

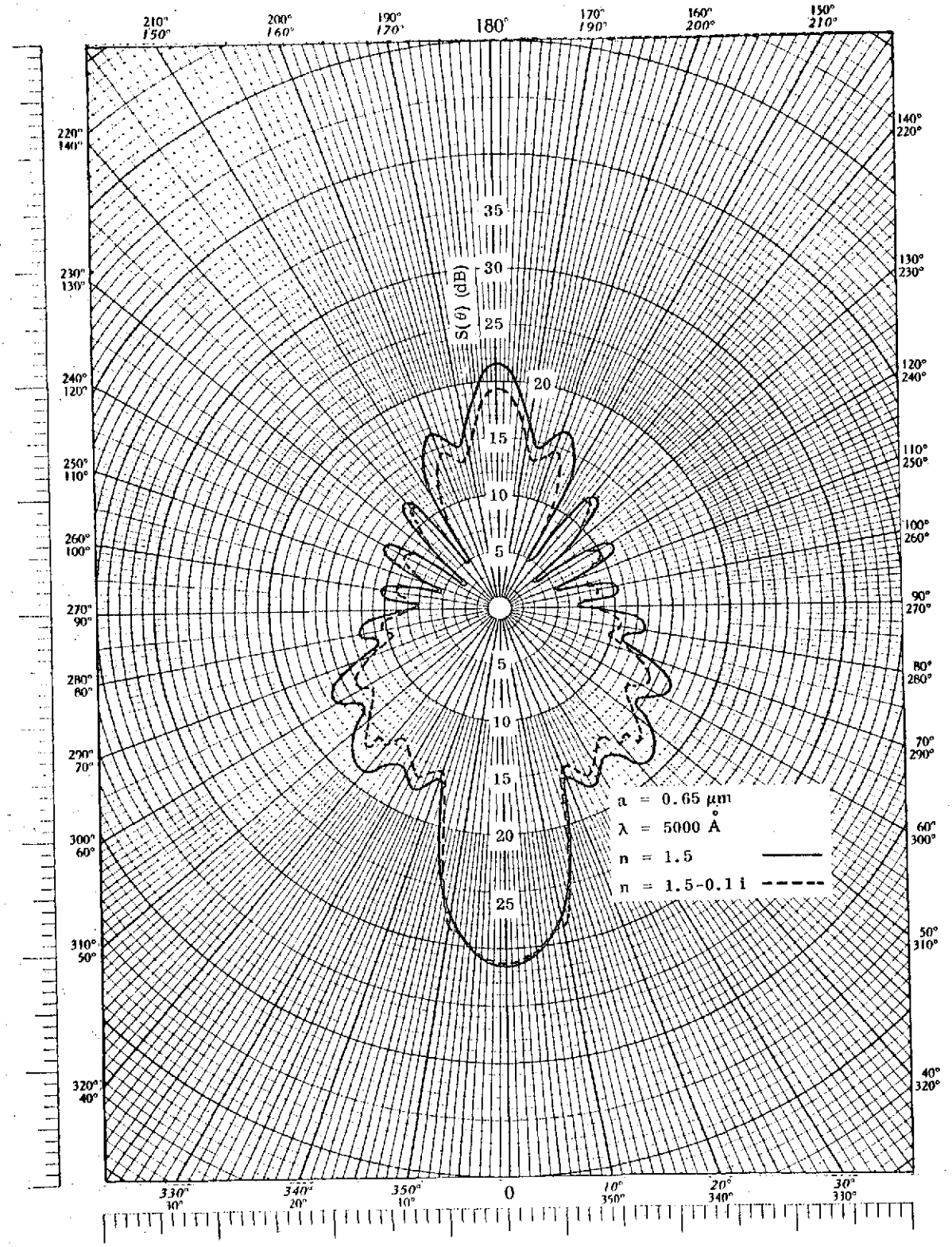

Figure A3 Angular dependence of scattering function, a=.65 μm, n=1.5, 1.5-.1

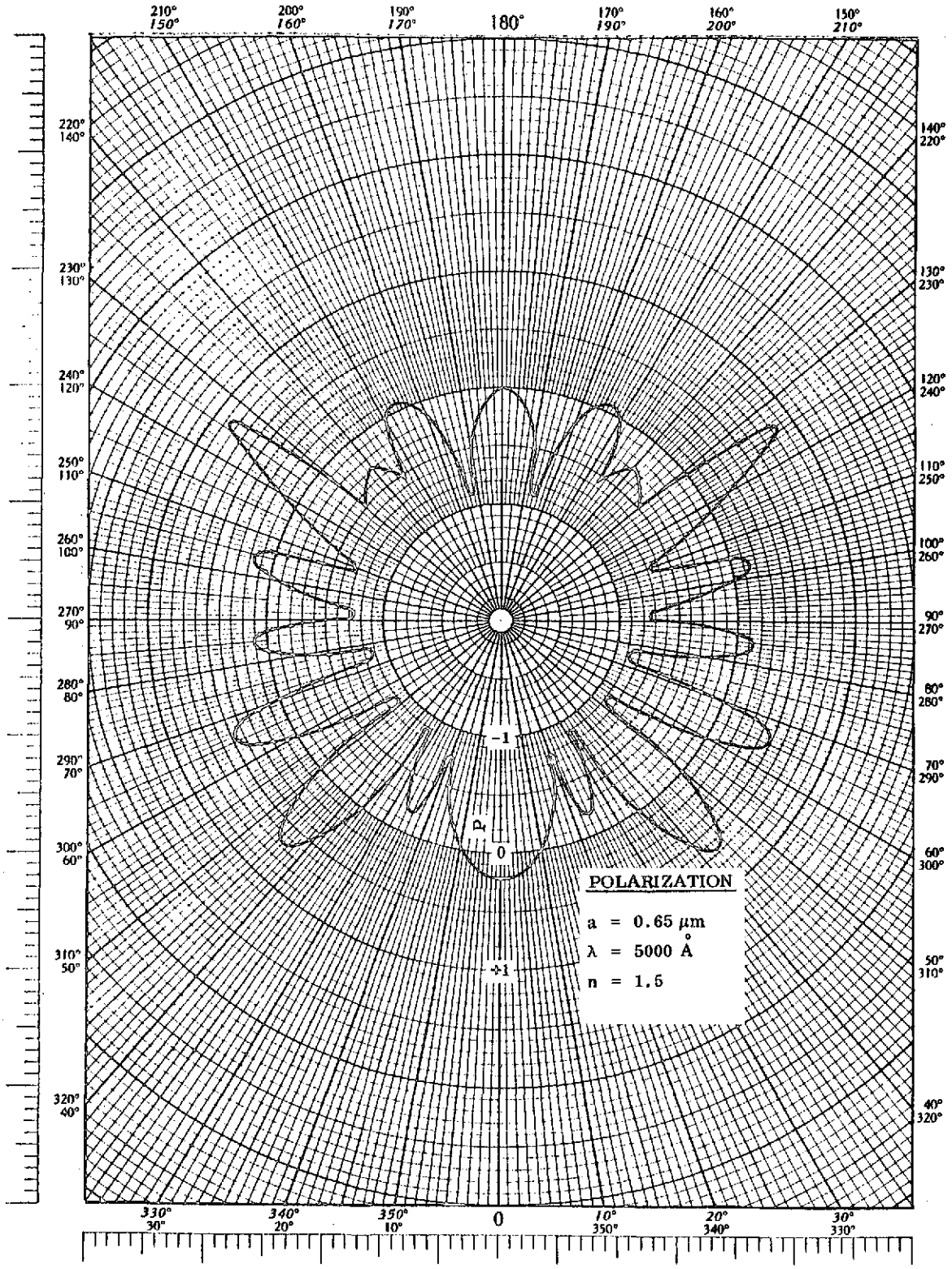

Figure A4 Angular dependence of polarization, a= .65μm, n= 1.5.

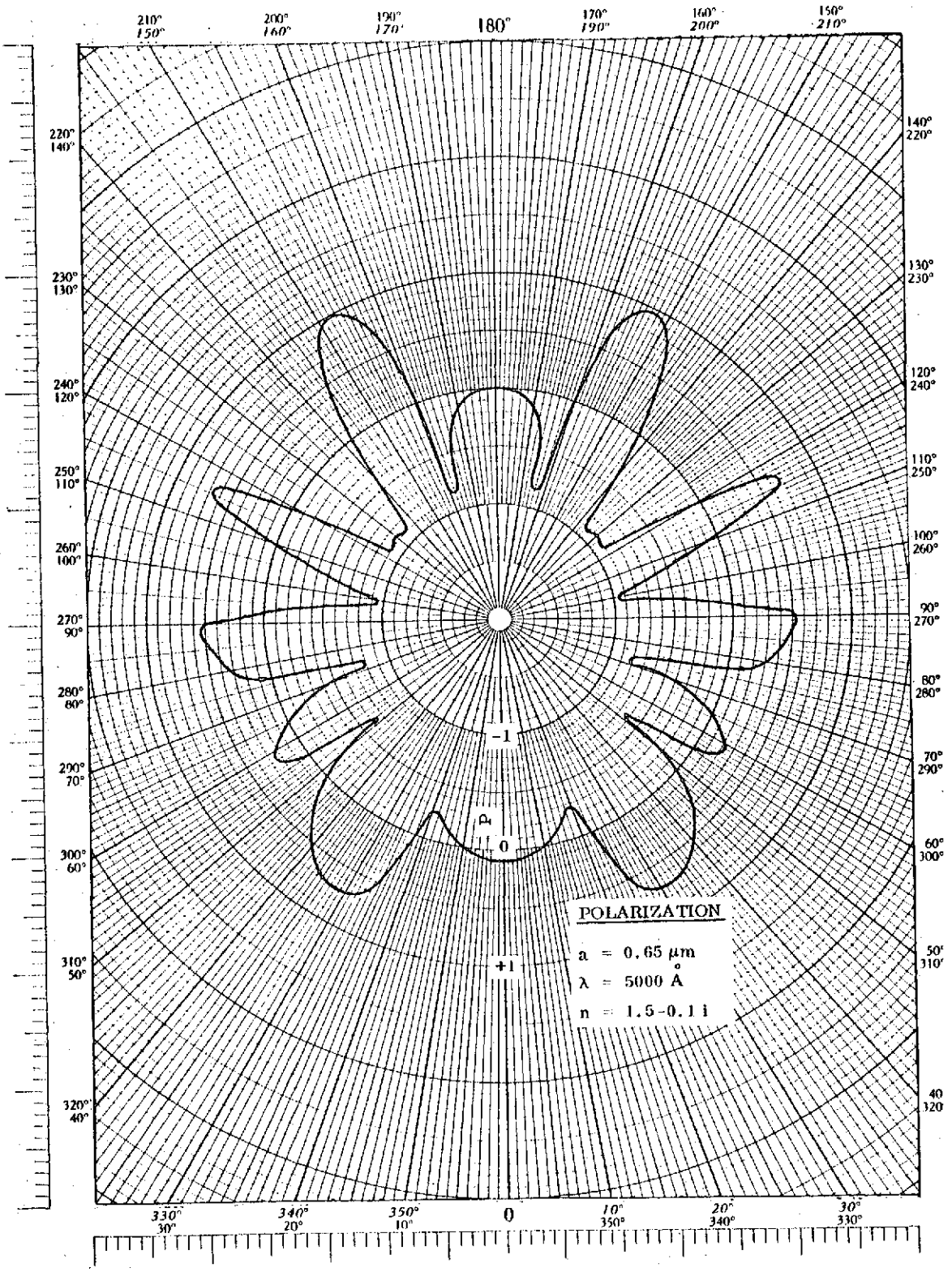

Figure A5 Angular dependence of polarization, a= .65μm, n= 1.5-.1 i.

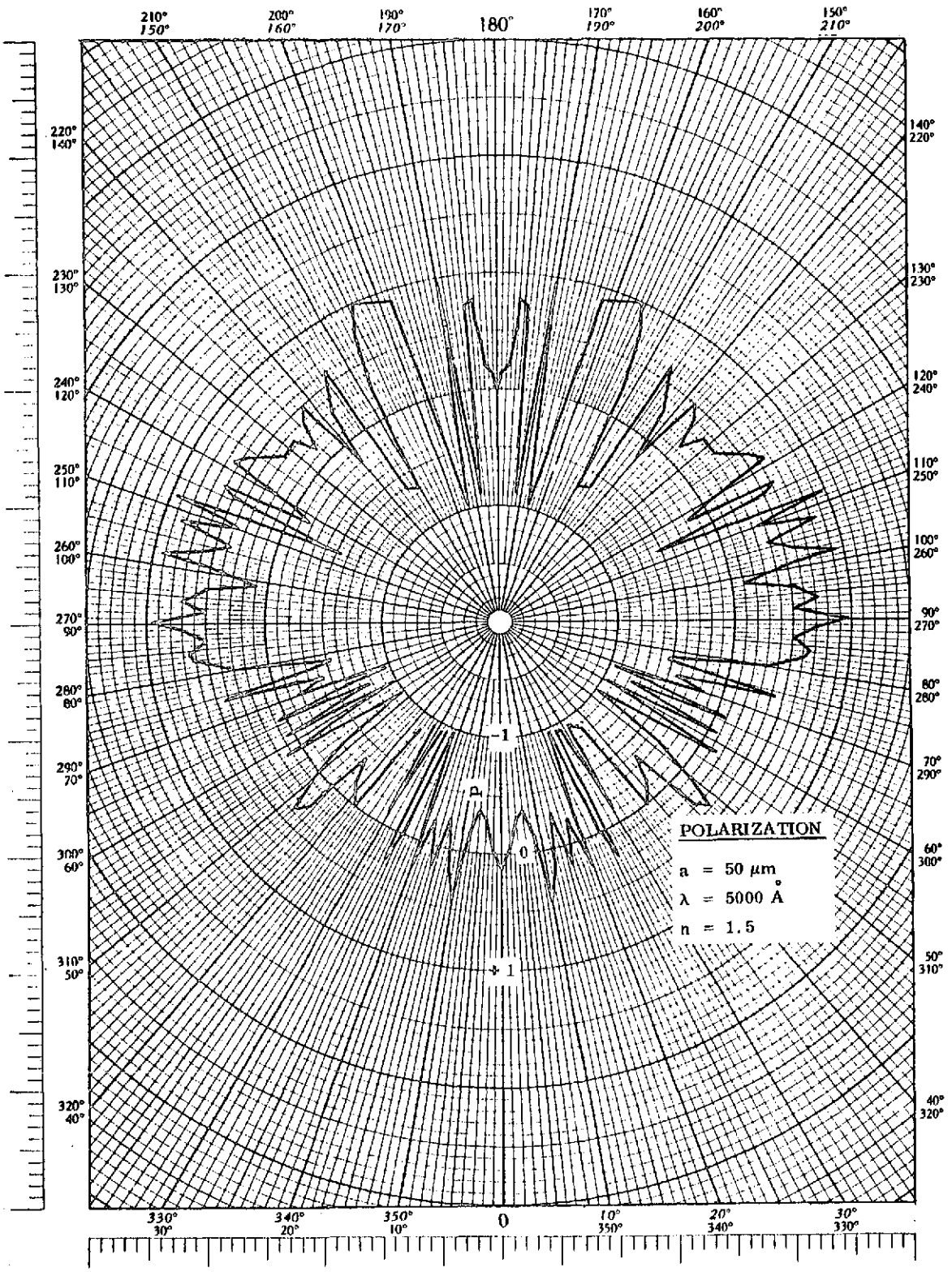

Figure A6 Angular dependence of polarization, a= .50μm, n= 1.5.

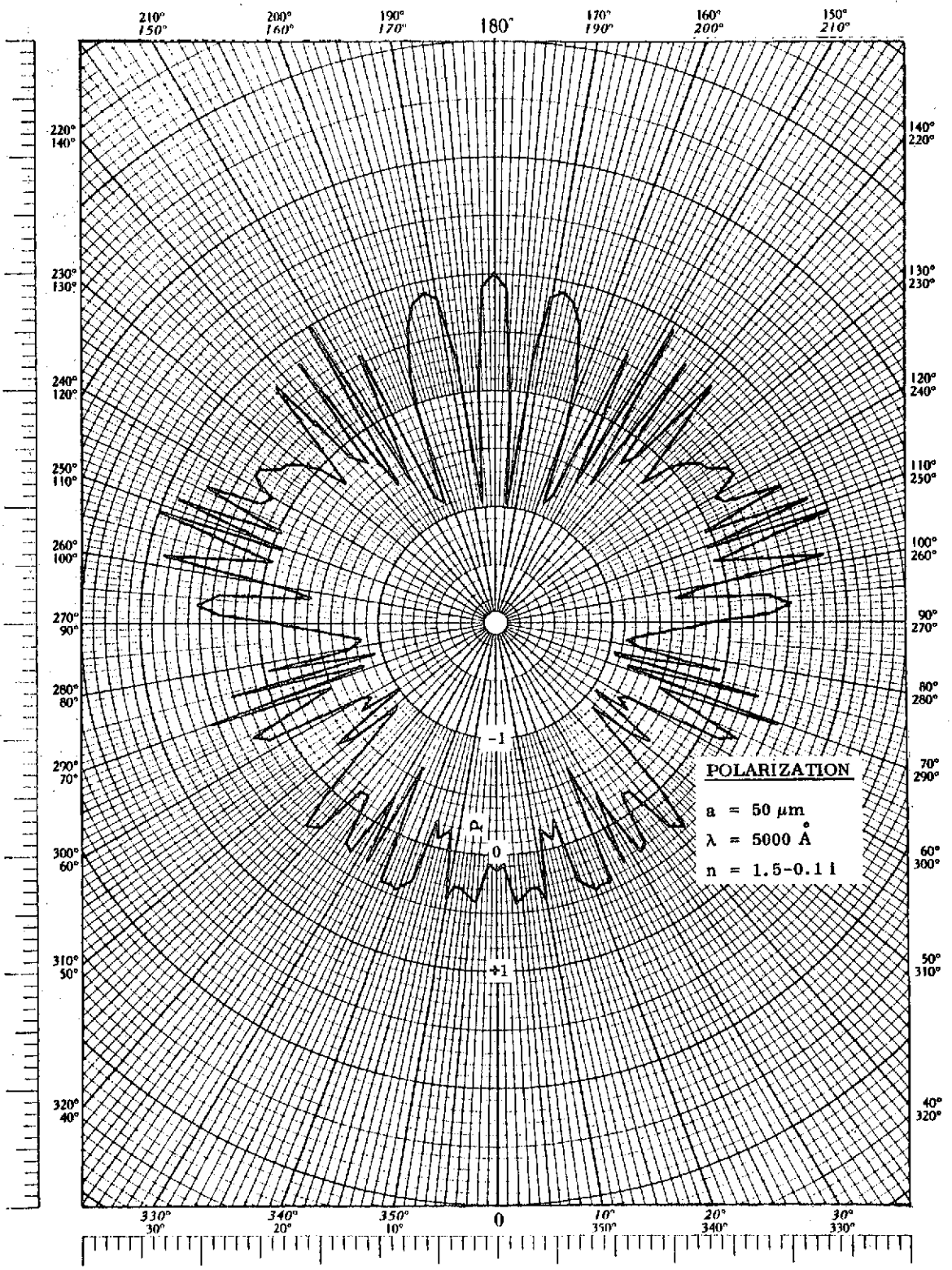

Figure A7 Angular dependence of polarization, a= 50μm, n= 1.5-.1 i.

APPENDIX B

CALCULATION OF COLUMN DENSITIES

The number of particles N passing through a spherical surface at a distance R from the center of the nucleus during a time Δt is given by

$$N = \sum_i P_i \, \Delta t = \sum_i n_i(R) \, v_i \, \Delta t \, 4\pi R^2, \tag{B-1}$$

where P_i, n_i and v_i are the production rate, the number density and the terminal velocity, respectively, of the particles in the ith size range.

The number density as a function of R is then given by

$$n_i(R) = \frac{P_i}{v_i \, 4\pi R^2} . \tag{B-2}$$

The column density of particles n_{col} is obtained by integrating Eq. (B-2) from R_{min} to R_{max}:

$$n_{col} = \sum_i \int_{R_{min}}^{R_{max}} \frac{P_i \, dR}{4\pi \, v_i R^2} . \tag{B-3}$$

R_{min} is the radius of the nucleus (R_n), and since v_i is constant for $R > 10 \, R_n$, the value of n_{col} is insensitive to the value of R_{max}. Equation (B-3) is actually the lower limit to n_{col}, since for $R < 10 \, R_n$ the particle velocities are less than v_i. The calculations of Delsemme and Miller (1971), shown in their Figure 2, suggest that the particles are subject to approximately constant acceleration until they move at nearly terminal

velocity. The integral in equation (B-3) is most sensitive to the particle velocities at small R. As an upper limit to n_{col}, suppose the actual particle velocities are given by

$$v(R) = \begin{cases} v_o & R_n \leq R < 10\ R_n \\ v_i & R \geq 10\ R_n \end{cases} . \qquad \text{(B-4)}$$

Here v_o is the initial velocity at which particles are ejected from the nucleus. The column density for species i is then

$$n_{col} = \frac{P_i}{4\pi\ R_n v_i} [0.1 + 0.9(v_i/v_o)]. \qquad \text{(B-5)}$$

Taking $v_o = 0.1\ v_i$ gives a column density 9.1 times the value obtained from equation (B-3) assuming $v = v_i$ everywhere. We could, of course, go on to evaluate equation (B-3) using the assumption of constant acceleration to obtain somewhat better estimates for n_{col}, but the results depend on the unknown ejection velocity v_o. For the present, we simply point out this refinement which should be included in more comprehensive models.

For calculating impacts suffered by a spacecraft passing near the comet, we have evaluated the column density for a linear path passing within R_o km of the nucleus (we will call this the impact parameter). The complications discussed above are not encountered because $R_o \gg R_n$. The spatial density is given by equation (B-2), and the column density is

$$n_{col}(a, R_o) = \frac{P(a)}{4v(a)R_o} . \qquad \text{(B-6)}$$

Since $v(a) \rightarrow 0$ as $a \rightarrow a_{max}$, the production rate $P(a)$ must also go to zero in order to avoid a singularity. Since the terminal velocity for $a > 10^{-4}\ a_{max}$ is given by

$$v(a) \simeq 2.88 \times 10^{-3}\ (a/a_{max})^{-1/2}[1-(a/a_{max})^{1/2}]\ \text{km/sec} \qquad \text{(B-7)}$$

(from Delsemme and Miller, 1971), we cut off the production rate by a factor $[1-(a/a_{max})^{1/2}]$. This does not affect the results presented in Section III. The production rate for $a > 4.44 \times 10^{-3}$ cm is given by

$$P(a) = 7.298 \times 10^{-4}\ \dot{M}_{dust}\ a^{-5}[1-(a/a_{max})^{1/2}]\ \text{sec}^{-1} \qquad \text{(B-8)}$$

where $\dot{M}_{dust} \simeq 5 \times 10^{4}$ g sec^{-1} and $a_{max} = 15.5$ cm at heliocentric distance 0.8 AU, while $\dot{M}_{dust} \simeq 2.77 \times 10^{5}$ g sec^{-1} and $a_{max} = 98.2$ cm at 0.34 AU (perihelion).

Using equations (B-7) and B(-8) in equation (B-6), then integrating over particle sizes from a to a_{max}, we obtain the cumulative column density:

$$n(a,R_o) \equiv \int_{a}^{a_{max}} n_{col}\ da \qquad \text{(B-9)}$$

$$= 1.813 \times 10^{-7}\ \frac{\dot{M}_{dust}}{a_{max}^{1/2}\ R_o}\ [\ a^{-3.5} - a_{max}^{-3.5}]; \qquad \text{(B-10)}$$

this represents the number of particles which have radii a or larger. Table B-I gives representative values.

TABLE B-I. Column Densities For an Impact Parameter of 100 km

Heliocentric Distance (AU)	n(a, 100 km) (cm^{-2})		
	$a = 10^{-2}$ cm	$a = 10^{-1}$ cm	a = 1 cm
0.34	5.1×10^{-3}	1.6×10^{-6}	5.1×10^{-10}
0.8	2.3×10^{-3}	7.3×10^{-7}	2.3×10^{-10}

For given values of a and R_o, n varies approximately inversely as the heliocentric distance because $\dot{M}_{dust}$ and a_{max} both vary approximately as r^{-2}.

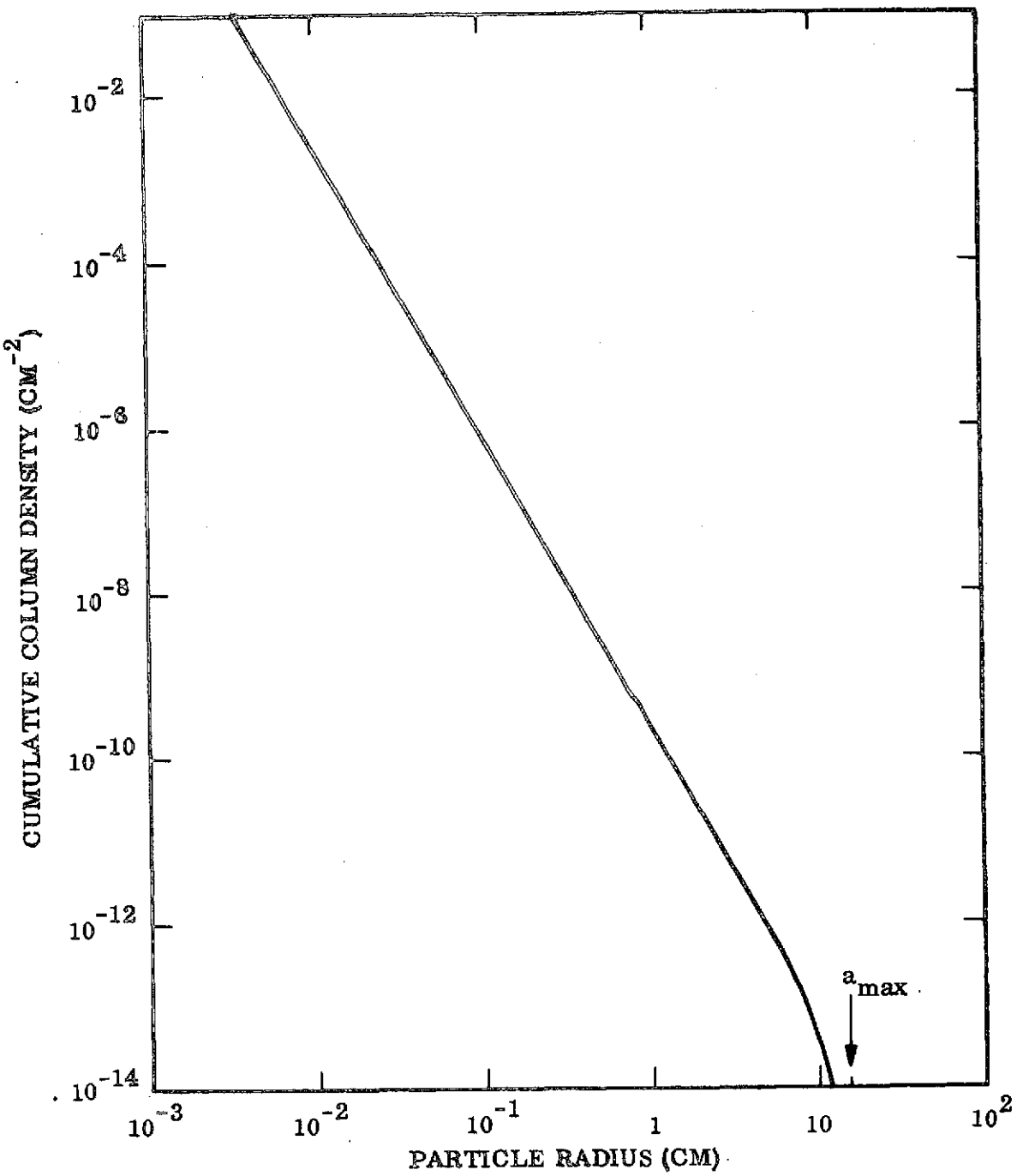

Figure B1 Cumulative column density vs. particle radius.